Gamma-Ray Emission from Protostellar Jets

From Candidates to Sources

Anabella Araudo[1],

(1) Institute of Physics, Czech Academy of Sciences

In collaboration with A. Marcowith, C. Carrasco-Gonzalez, A. Rodriguez-Kamenetzky, L.F. Rodriguez, M. Padovani, A.L Muller, O. Tunc, M.V. del Valle, B. Gatches, F. Suzuki Vidal, A. Gintrand, Q. Moreno

Workshop: Kinetic Physics from Astrophysical Plasmas (KPAP)
Montpellier, 18-19 May, 2026

Table of contents

Introduction

Star forming regions

Protostellar jets

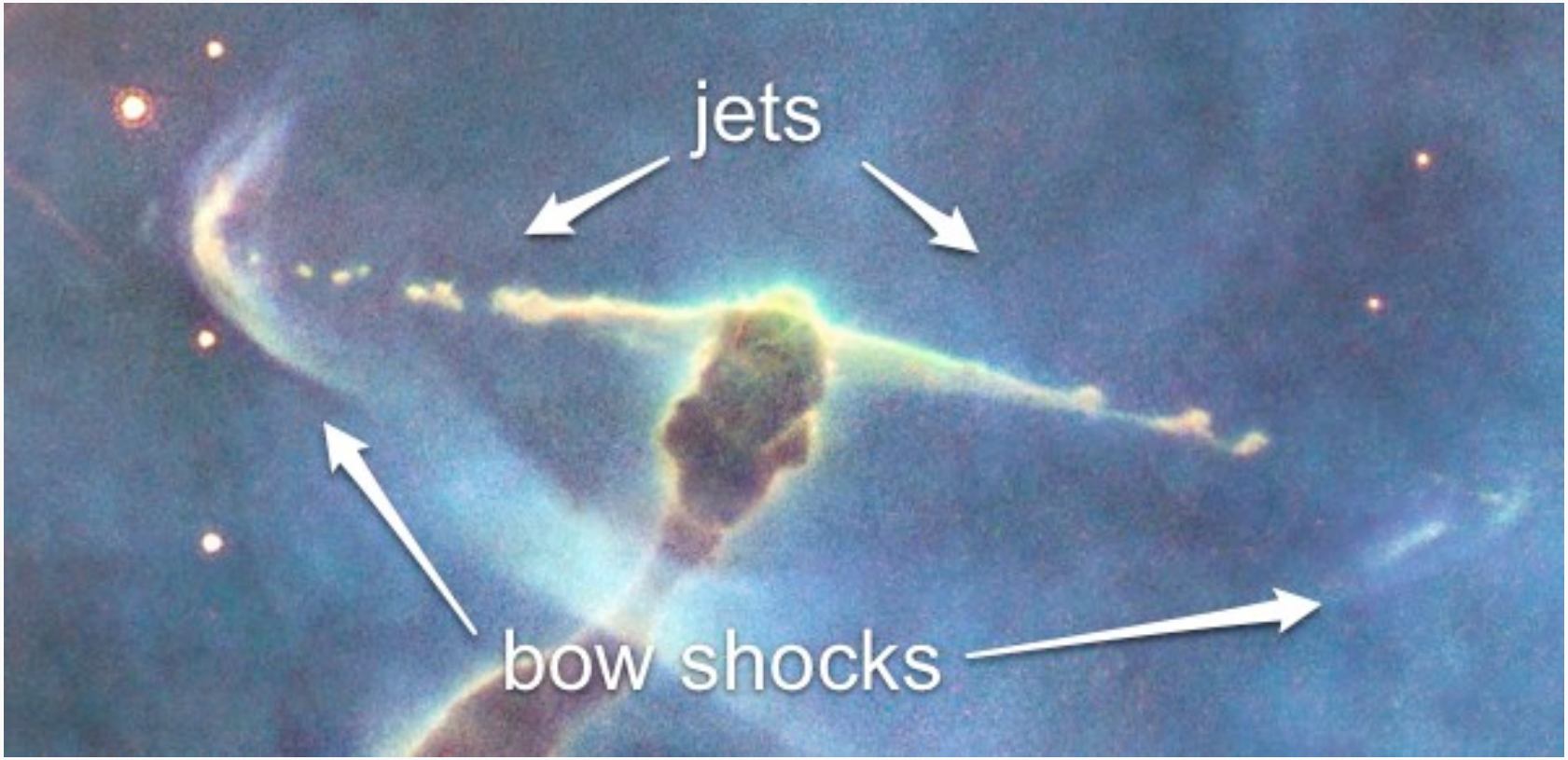

Young Stellar Objects (YSOs)

- Central protostar
- Accretion disc
- Fast and collimated jets

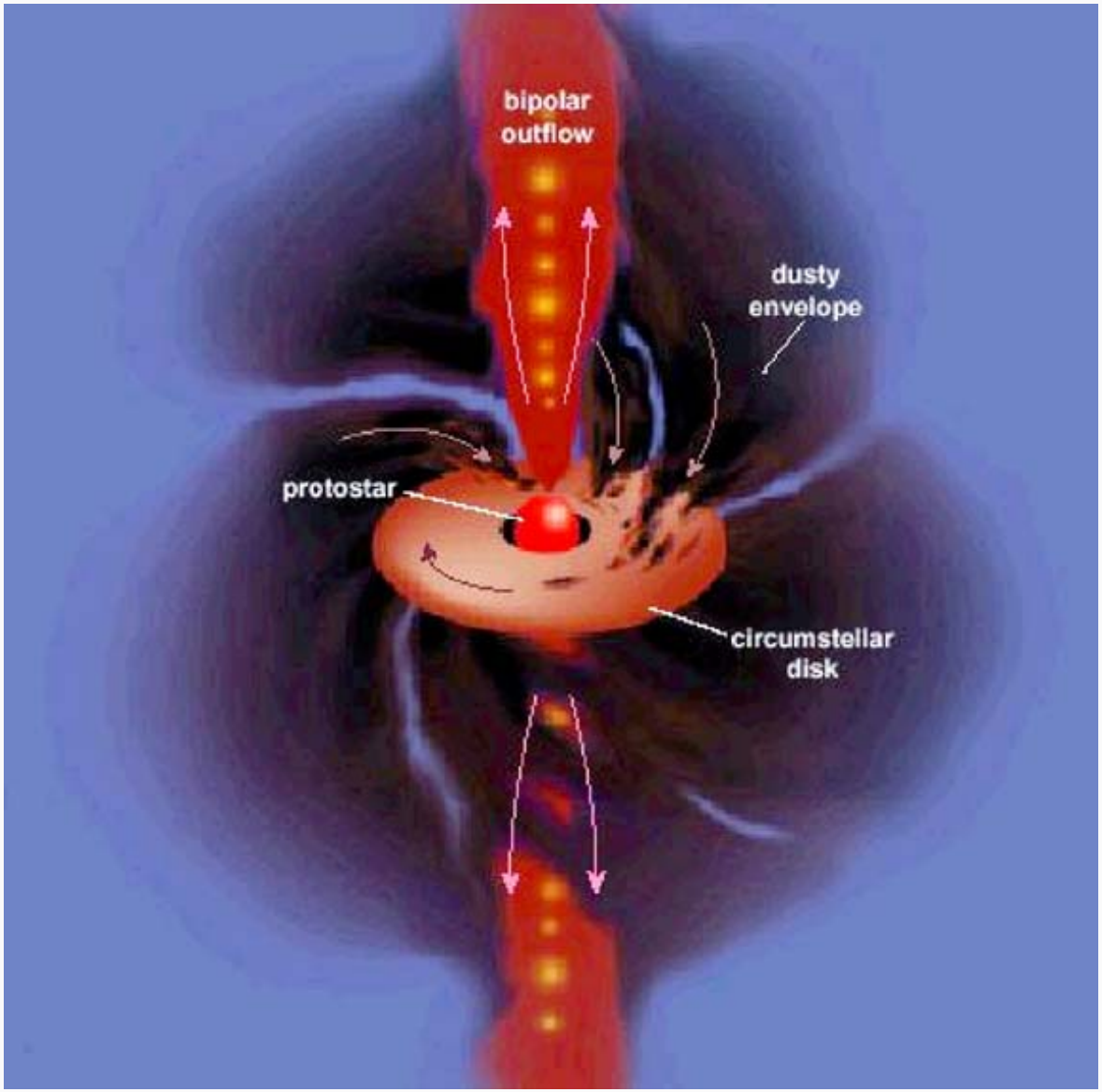

Jet velocity inferred from proper motions

- Low-mass protostars:
  $v_j \sim 50 - 200$ km/s
- High-mass protostars:
  $v_j \sim 200 - 1500$ km/s

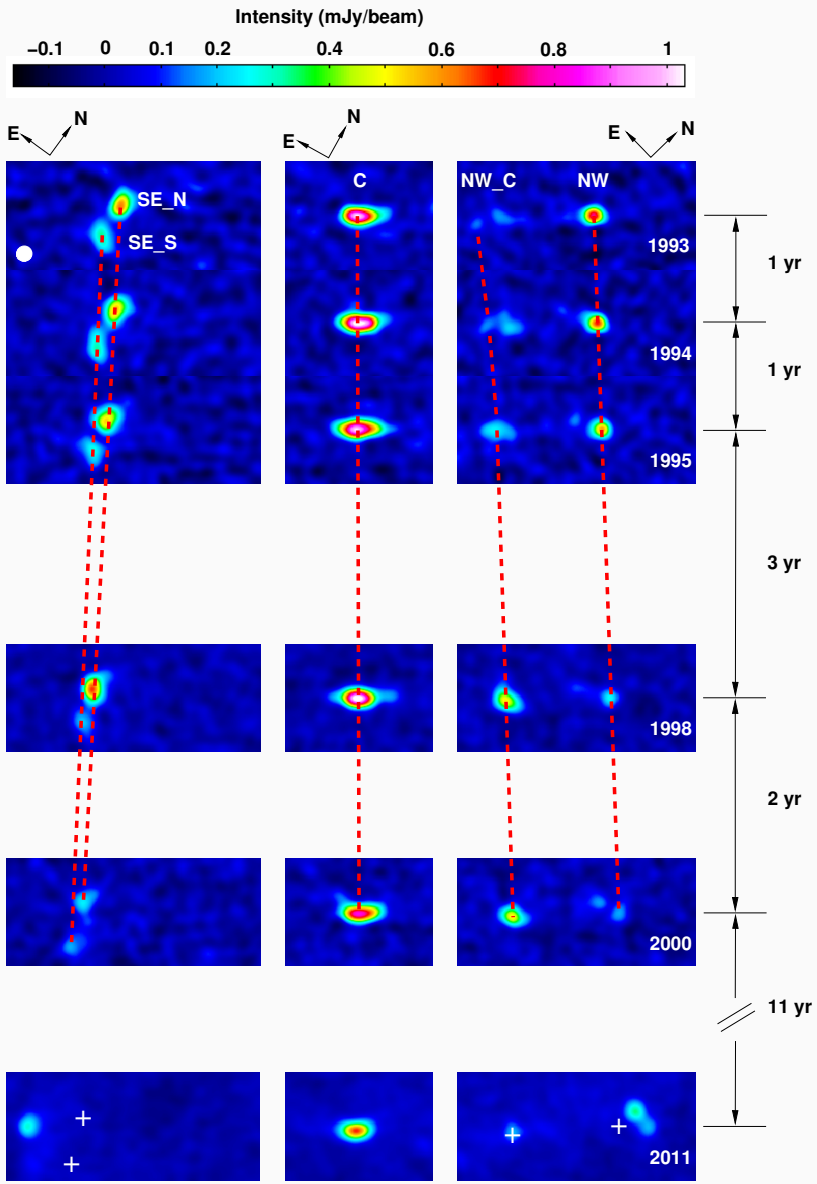

Rodriguez-Kamenetzky et al. (2016)

The inner jet in HH 211 ($M_\star \sim 0.06\,M_\odot$)

ALMA observations show that the jet is launched at ~ 0.021 AU in the disc with a velocity ~ 107 km s^{-1} (Lee et al. 2025)

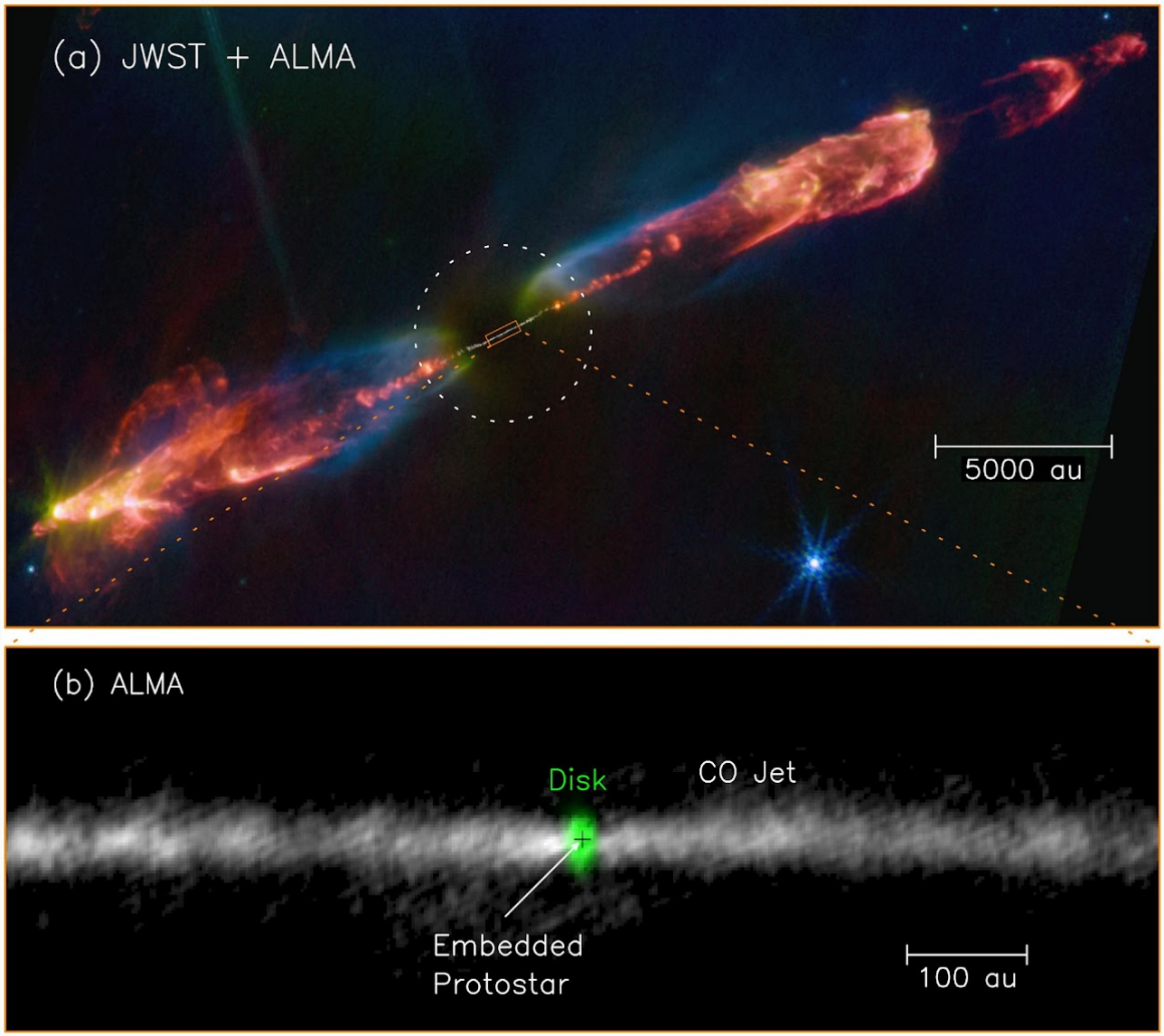

Thermal and non-thermal emission

- Well known thermal emitters
- Increasing population of **non-thermal protostellar jets** (e.g. Purser et al. 2016)

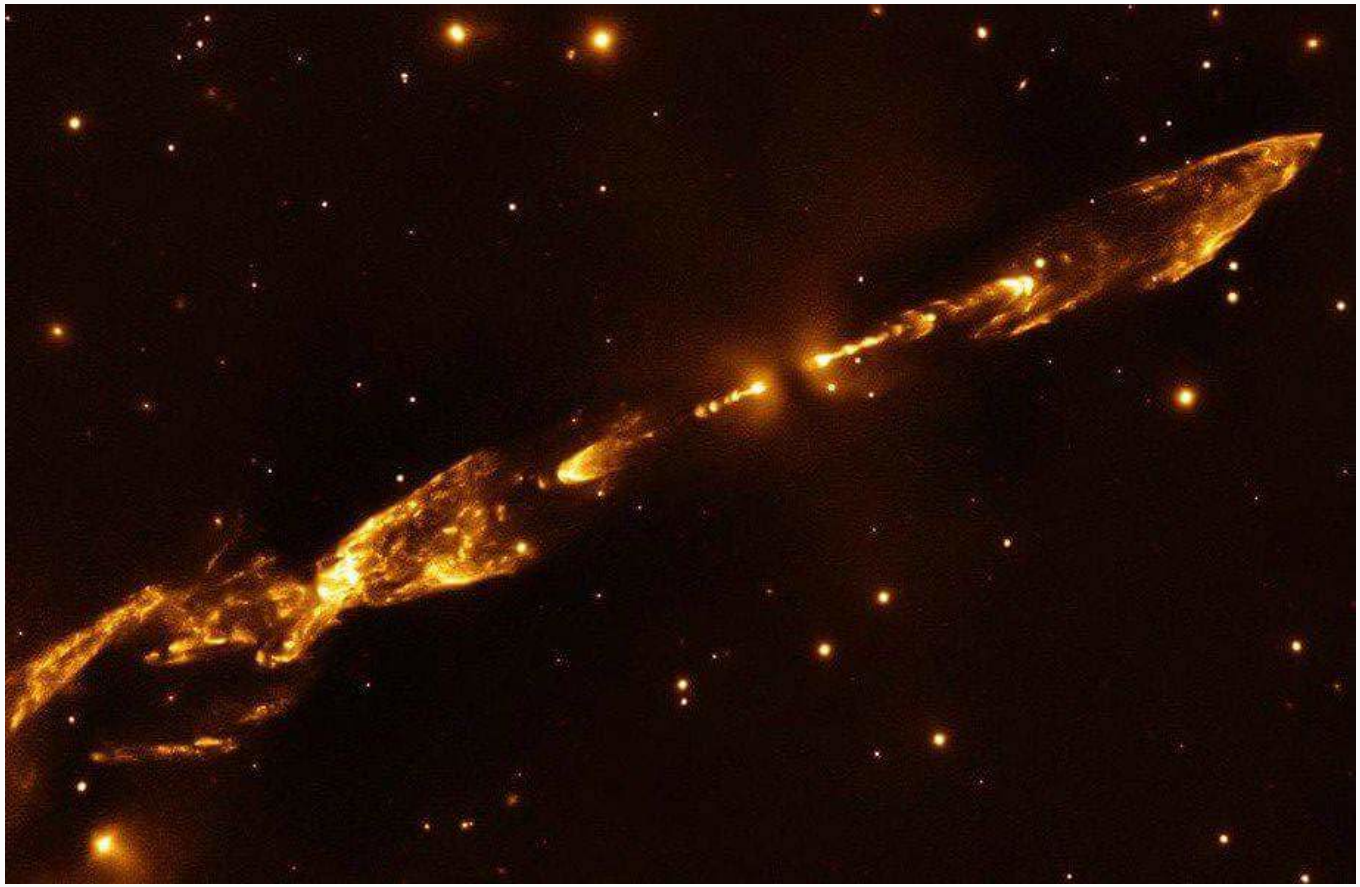

HH 212 - Hubble Space Telescope

Non-thermal (synchrotron) emission from protostellar jets

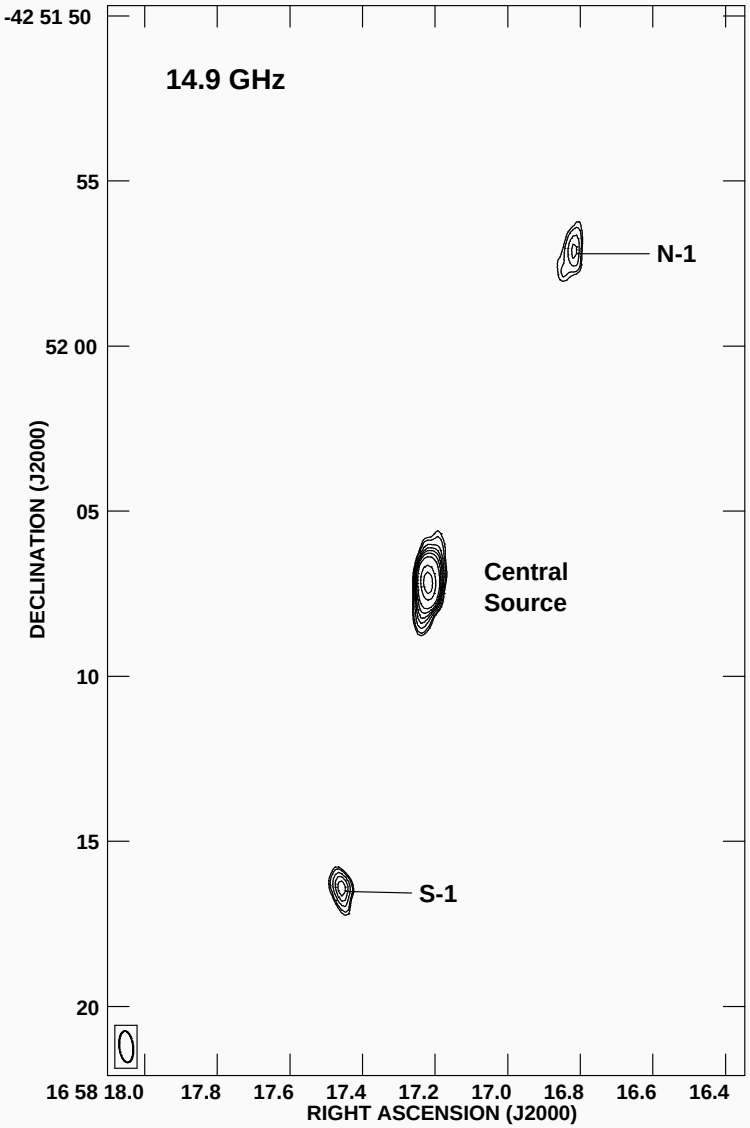

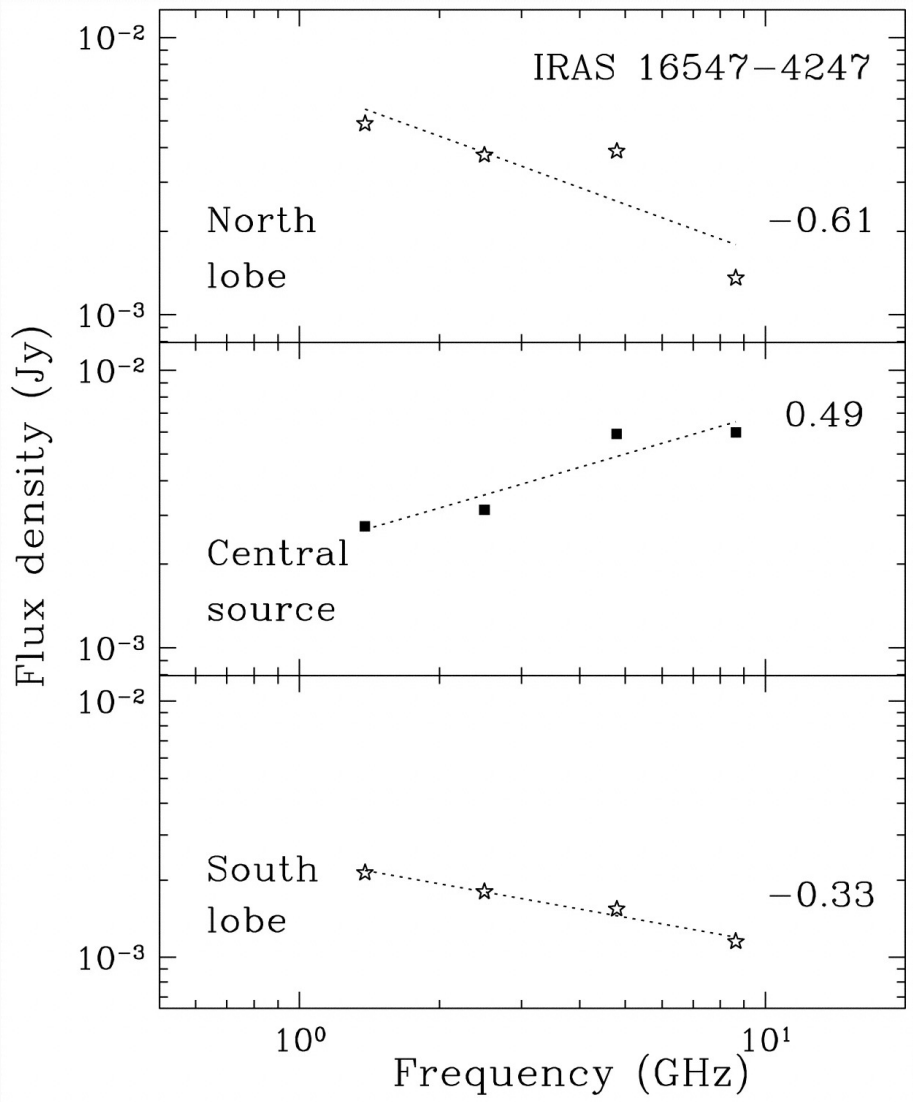

Rodríguez et al. (2005)

Garay et al. (2003)

Jet density

Mass conservation across the jet:

$$\frac{n_{\dot{M}}}{\mathrm{cm}^{-3}} \approx 150 \left(\frac{\dot{M}_\mathrm{i}}{10^{-6}\,\mathrm{M}_\odot\,\mathrm{yr}^{-1}}\right)\left(\frac{v_\mathrm{j}}{1000\,\mathrm{km\,s}^{-1}}\right)^{-1}\left(\frac{R_\mathrm{j}}{10^{16}\,\mathrm{cm}}\right)^{-2}$$

Upper limit given by free-free emission ($\epsilon_{ff} < \epsilon_\mathrm{synchr}$):

$$\frac{n_\mathrm{ff}}{\mathrm{cm}^{-3}} \approx 1.4 \times 10^5 \left(\frac{d}{\mathrm{kpc}}\right)\left(\frac{S_\nu}{\mathrm{mJy}}\right)^{\frac{1}{2}}\left(\frac{R_\mathrm{j}}{10^{16}\mathrm{cm}}\right)^{-\frac{3}{2}}\left(\frac{v_\mathrm{sh}}{1000\,\mathrm{km\,s}^{-1}}\right)^{\frac{1}{2}}$$

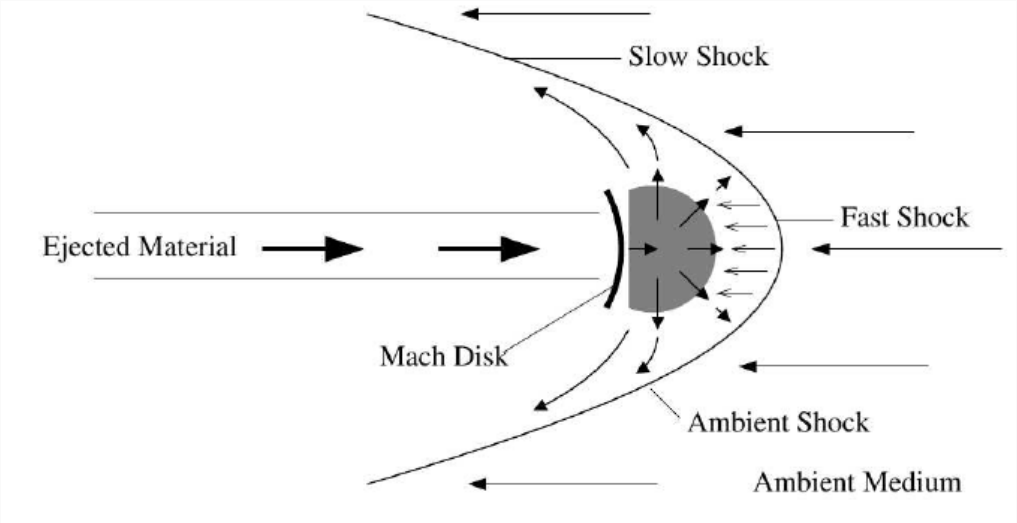

O'Sullivan (2009)

Magnetic fields and non-thermal particles content

$$\frac{U_{\rm e}}{\rm erg\,cm^{-3}} \sim 5{\times}10^{-8} \left(\frac{d}{\rm kpc}\right)^{2} \left(\frac{S_\nu}{\rm mJy}\right) \left(\frac{R_{\rm j}}{10^{16}\rm cm}\right)^{-3} \left(\frac{\nu}{\rm GHz}\right)^{\frac{s-1}{2}} \left(\frac{B_{\rm s}}{\rm mG}\right)^{-\frac{s+1}{2}}$$

	Source	
(1)	G263.74	N
(2)	G263.7759	NW
(3)	G310.1420	A4
(4)		D
(5)	G313.7654	A2
(6)		D
(7)	G339.8838	NE
(8)		SW
(9)	G343.1261	N4
(10)		S1
(11)	G114.0853	B

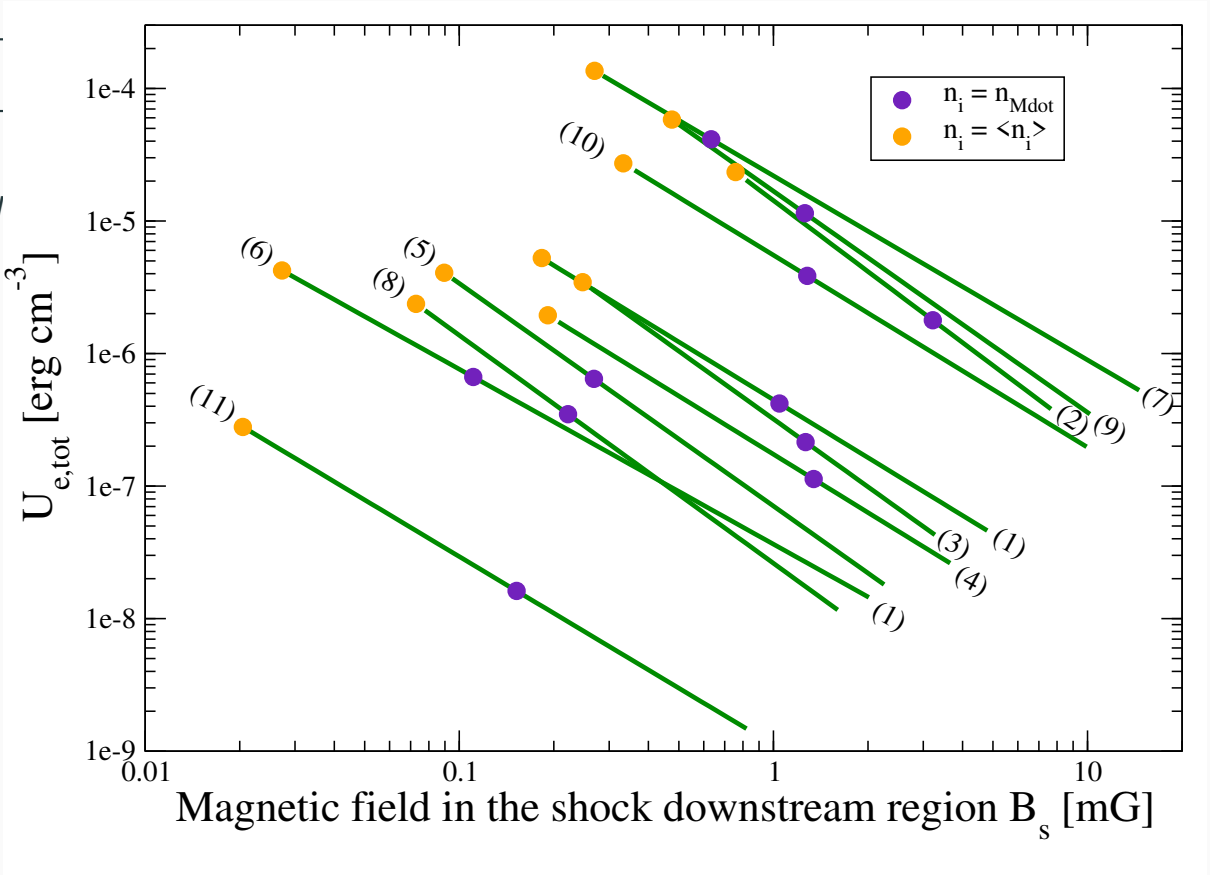

Araudo et al. (2021)

Radiative and adiabatic shocks

Radiative shocks ($l_{\rm th} < R_{\rm j}$): Compression of cosmic rays in the molecular cloud[1] (e.g. Chevalier 1999)

Adiabatic shocks ($l_{\rm th} > R_{\rm j}$): Local particle acceleration (Bell 1978)

Thermal cooling time:

$$t_{\rm th} = \frac{3}{2}\frac{k_B T_{\rm ps}}{n\lambda(T_{\rm ps})}$$

Thermal cooling length:

$$l_{\rm th} = t_{\rm th}\frac{v_{\rm sh}}{4}$$

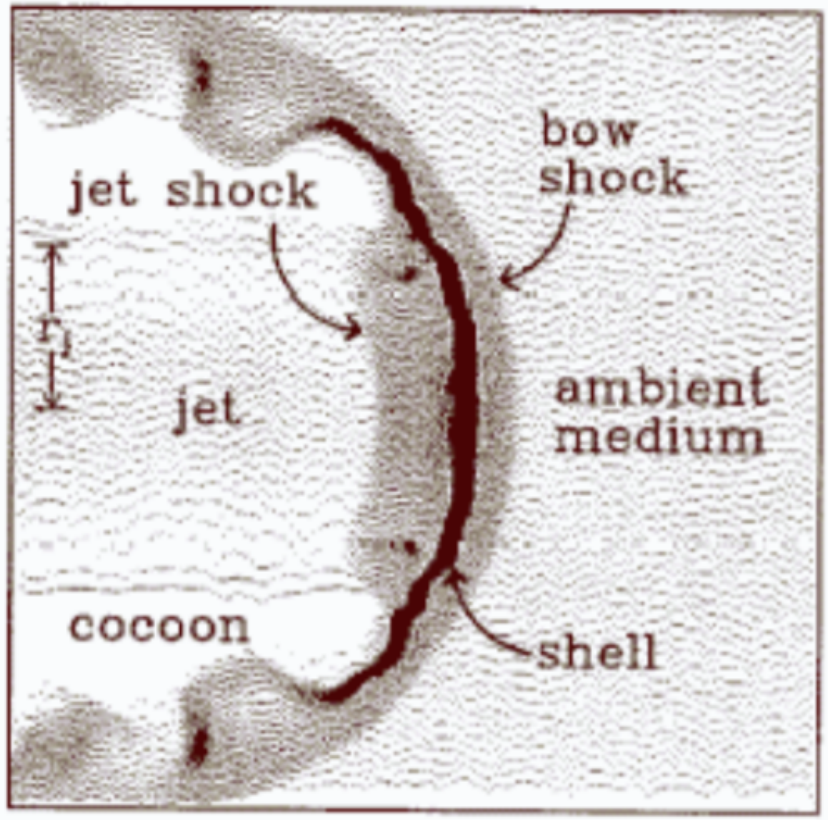

Blondin et al. (1989)

[1] As for old supernova remnants emitting synchrotron radiation in the radiative phase.

Adiabatic and radiative shocks

Thermal cooling length: $\frac{l_{\rm th}}{\rm cm} \simeq 6.9 \times 10^{16} \left(\frac{n_{\rm j}}{10^4\ {\rm cm^{-3}}}\right)^{-1} \left(\frac{v_{\rm sh}}{1000\ {\rm km\ s^{-1}}}\right)^{\frac{9}{2}}$

Critical shock velocity ($l_{\rm th} = R_{\rm j}$): $\frac{v_{\rm sh}}{\rm km\ s^{-1}} = 650 \left(\frac{n_{\rm j}}{10^4\ {\rm cm^{-3}}}\right)^{\frac{2}{9}} \left(\frac{R_{\rm j}}{10^{16}\ {\rm cm}}\right)^{\frac{2}{9}}$

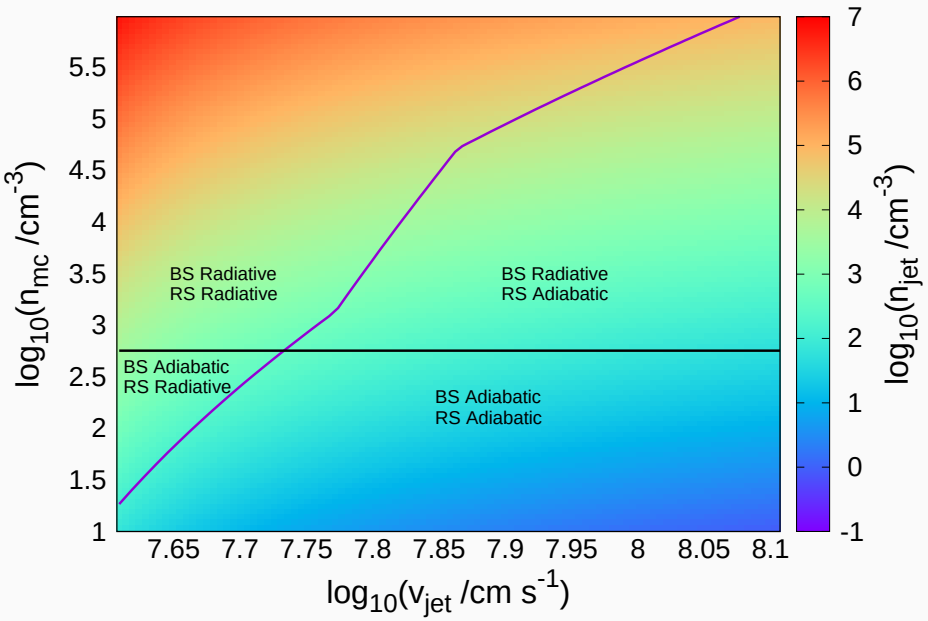

Araudo et al. (in prep.)

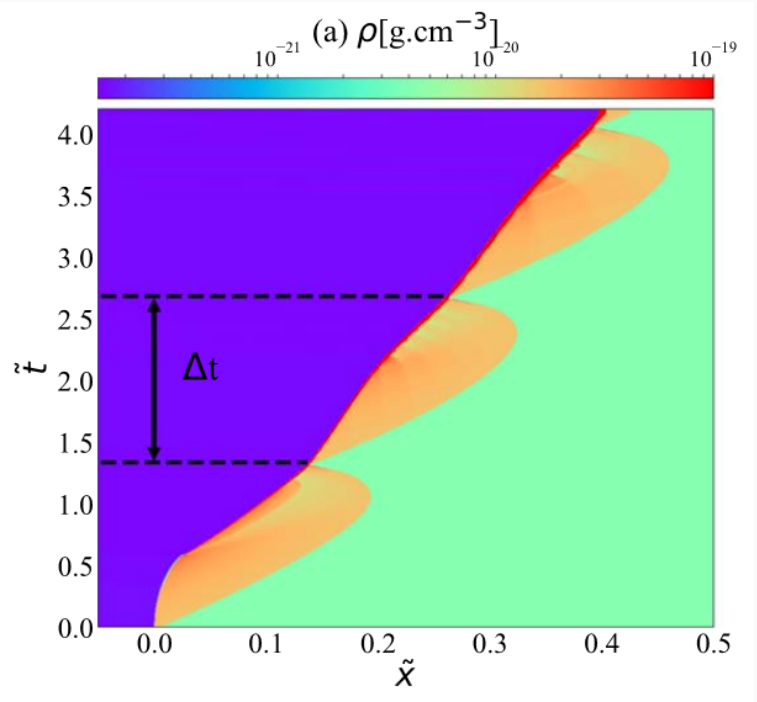

Gintrand et al. (2022)

Maximum energies and gamma-ray emission

Bell instabilities in YSO jets

Maximum growth rate:

$$\frac{\Gamma_{\rm max,NR}}{\rm s^{-1}} \sim 10^{-5} \left(\frac{\eta_p}{0.02}\right) \left(\frac{v_{\rm sh}}{1000\,{\rm km\,s^{-1}}}\right)^3 \left(\frac{n_i}{10^3\,{\rm cm^{-3}}}\right)^{\frac{1}{2}} \left(\frac{E_{\rm p}}{\rm GeV}\right)^{-1}$$

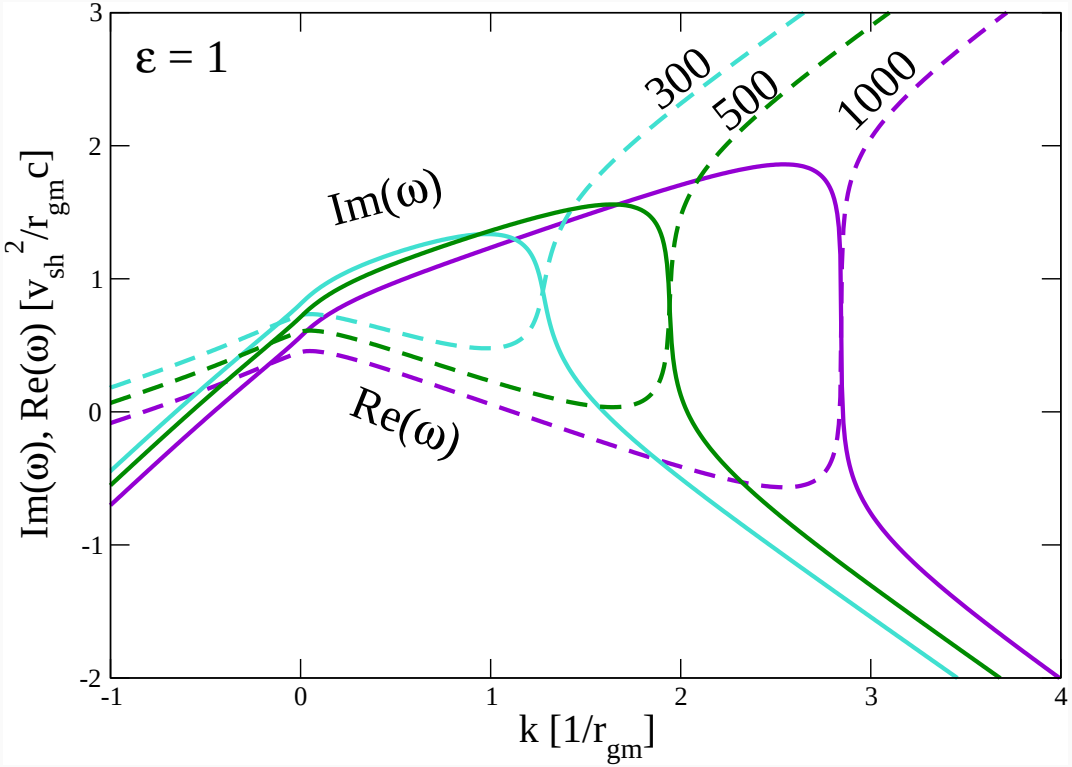

Araudo et al. (2021)

Protons maximum energy - $E_{p,\mathrm{max}}$

- $E_{p,\mathrm{max}}$ upper-limit due to the escape of particles upstream of the shock (Zirakashvili & Ptuskin 2008, Bell et al. 2013)
- For a distribution of protons $N_p \propto E_p^{-s}$

$$\Gamma_{\mathrm{max,NR}}\left(\frac{R_\mathrm{j}}{v_\mathrm{sh}}\right) > 5 \Rightarrow \frac{E_{p,\mathrm{max}}}{\mathrm{m_p c^2}} = \begin{cases} (2-s)F & s<2 \\ \log\left(\frac{E_{p,\mathrm{max}}}{\mathrm{GeV}}\right)^{-1} F & s=2 \\ \left[(s-2)\frac{1}{m_p c^2}F\right]^{\frac{1}{s-1}} & s>2 \end{cases}$$

$$F \simeq 65.83 \left(\frac{U_{p,\mathrm{tot}}}{10^{-5}\mathrm{erg\,cm^{-3}}}\right)\left(\frac{R_\mathrm{j}}{10^{16}\mathrm{cm}}\right)\left(\frac{n_i}{10^4\,\mathrm{cm^{-3}}}\right)^{-\frac{1}{2}}.$$

Gamma-ray emission

GeV-TeV protons (electrons) produce gamma-rays by proton-proton collisions (relativistic Bremsstrahlung)

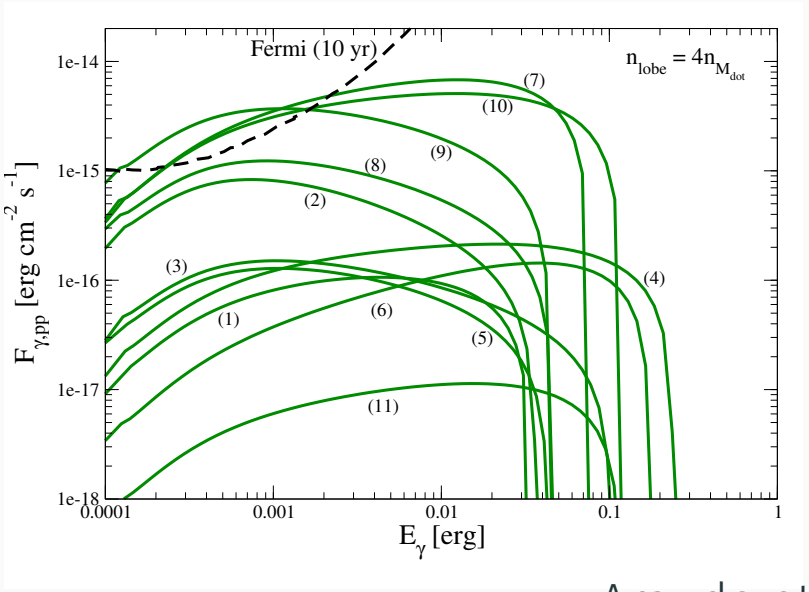

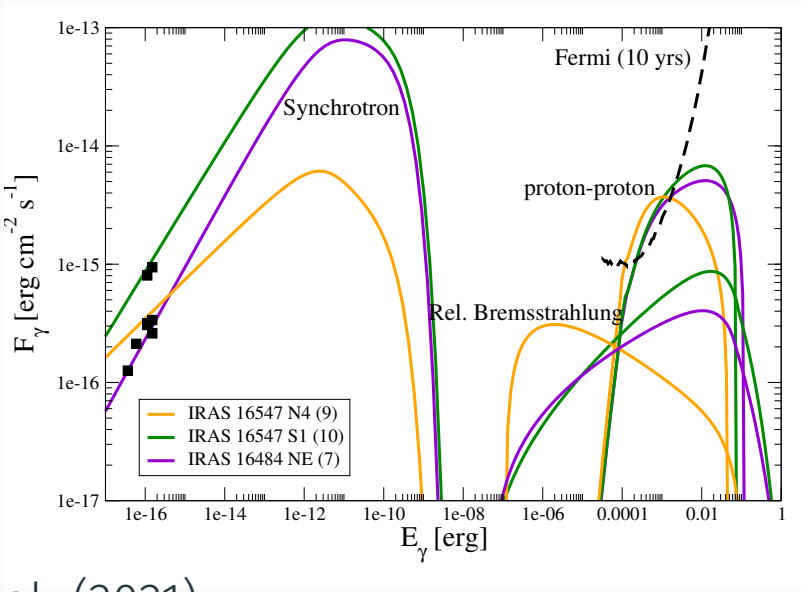

Araudo et al. (2021)

Density enhancement via Rayleigh-Taylor mixing[2]

$$\frac{n'_{\rm max}}{n_{\rm mc}} \sim 1000 \left(\frac{n_{\rm j}}{10^4\,{\rm cm}^{-3}}\right)^{\frac{1}{2}} \left(\frac{v_{\rm j}}{1000\,{\rm km\,s}^{-1}}\right) \left(\frac{B_{\rm mc,\perp}}{0.1{\rm mG}}\right)^{-1}$$

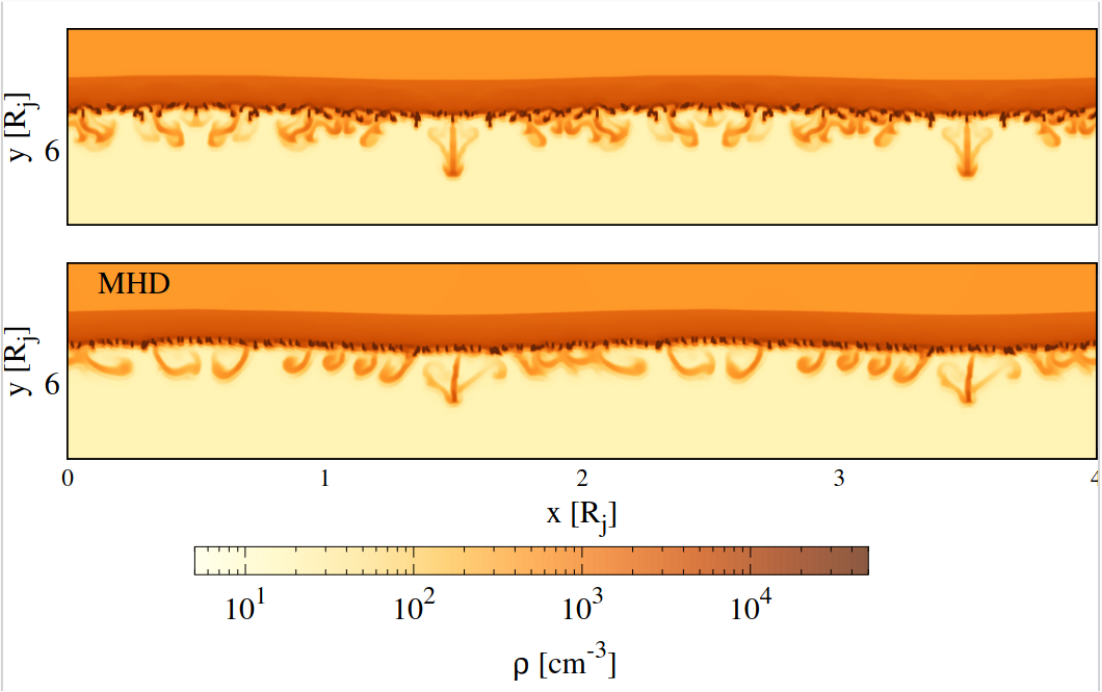

del Valle, Araudo & Suzuki-Vidal (2022)

[2]Self-similar solutions for the dynamics of the collision between radiative and adiabatic planar shocks (Gintrand, Moreno, Araudo, Tikhonchuk & Weber, 2021)

Gamma-ray emission from HH80-81

Herbig Haro (HH) objects HH80 and HH81

Located where the southern jet from the massive protostar IRAS 18162-2048 terminates. Due to their proximity ($d = 1.4$ kpc) and because these HH objects are located at the edge of the molecular cloud in which they are embedded, these sources are very well observed along the electromagnetic spectrum, from radio to X-rays.

Herbig-Haro 80/81. Credit: NASA, ESA, and B. Reipurth

IRAS 18162-2048 (HH80/HH81)

- $M_\star \sim 20 M_\odot$
- $L_{\rm bol} \sim 10^4 L_\odot$
- $d = 1.7$ kpc
- $v_{\rm j} \sim 1000$ km/s

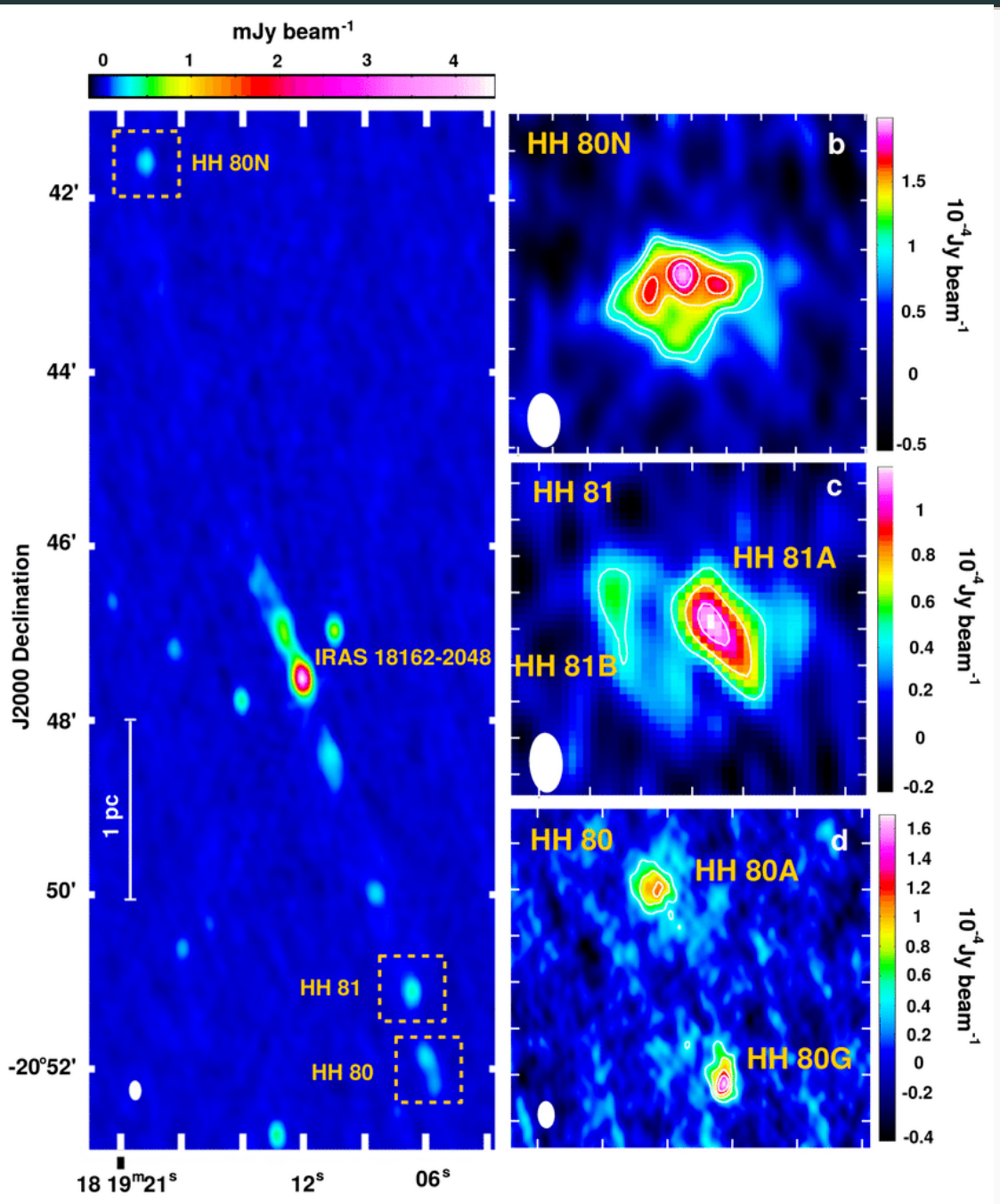

HH80-81 associated to 4FGL J1818.5−2036

4σ detection significance

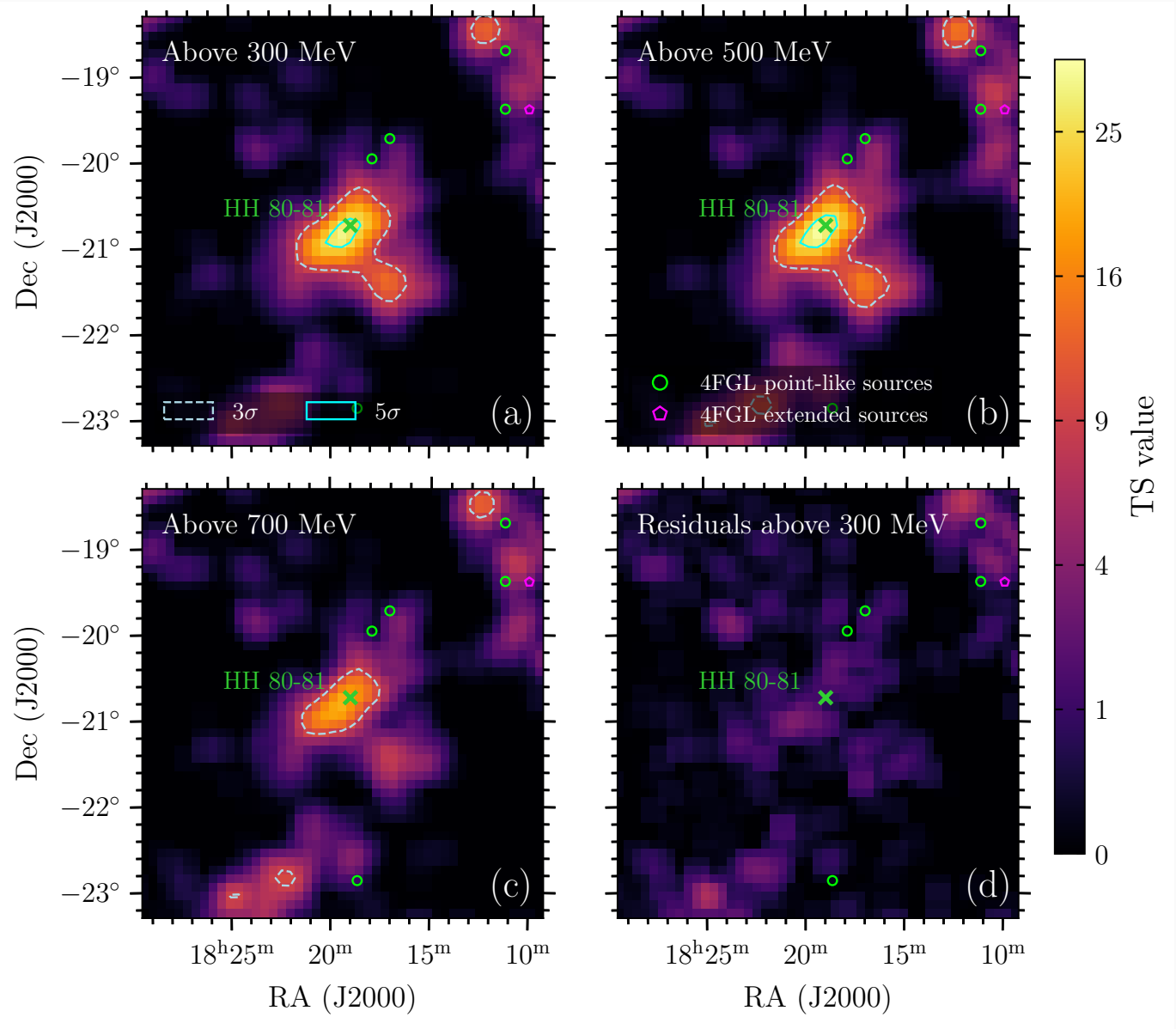

Mendez-Gallego et al. (2025)

Spectral energy distribution

Best fitting parameters:

- $\Gamma_{e,p} = 2.62$
- $n = 100\ \mathrm{cm}^{-3}$
- $E_{e,max} = 3$ TeV
- $E_{p,max} = 12$ TeV

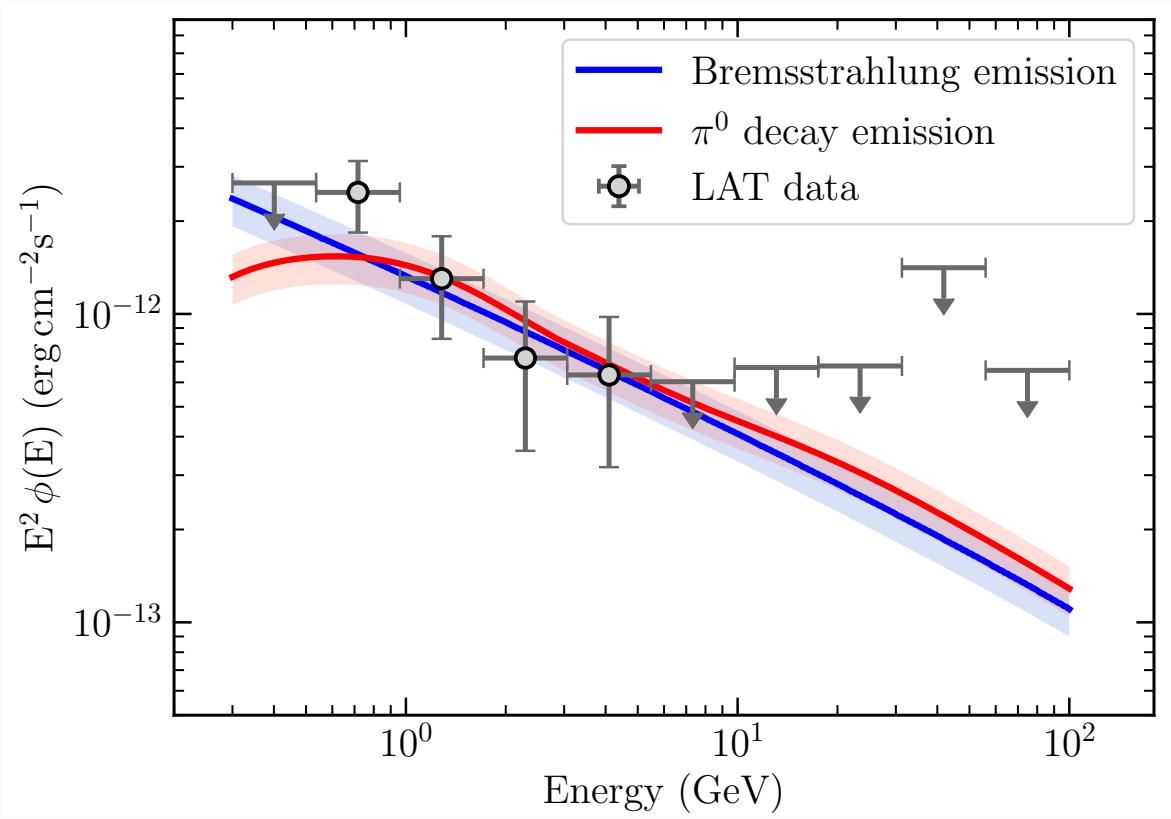

Mendez-Gallego et al. (2025)

Note however that $\alpha_{\mathrm{GHz}} = 0.3 \Longrightarrow \Gamma_e = 1.6$

Thermal contamination

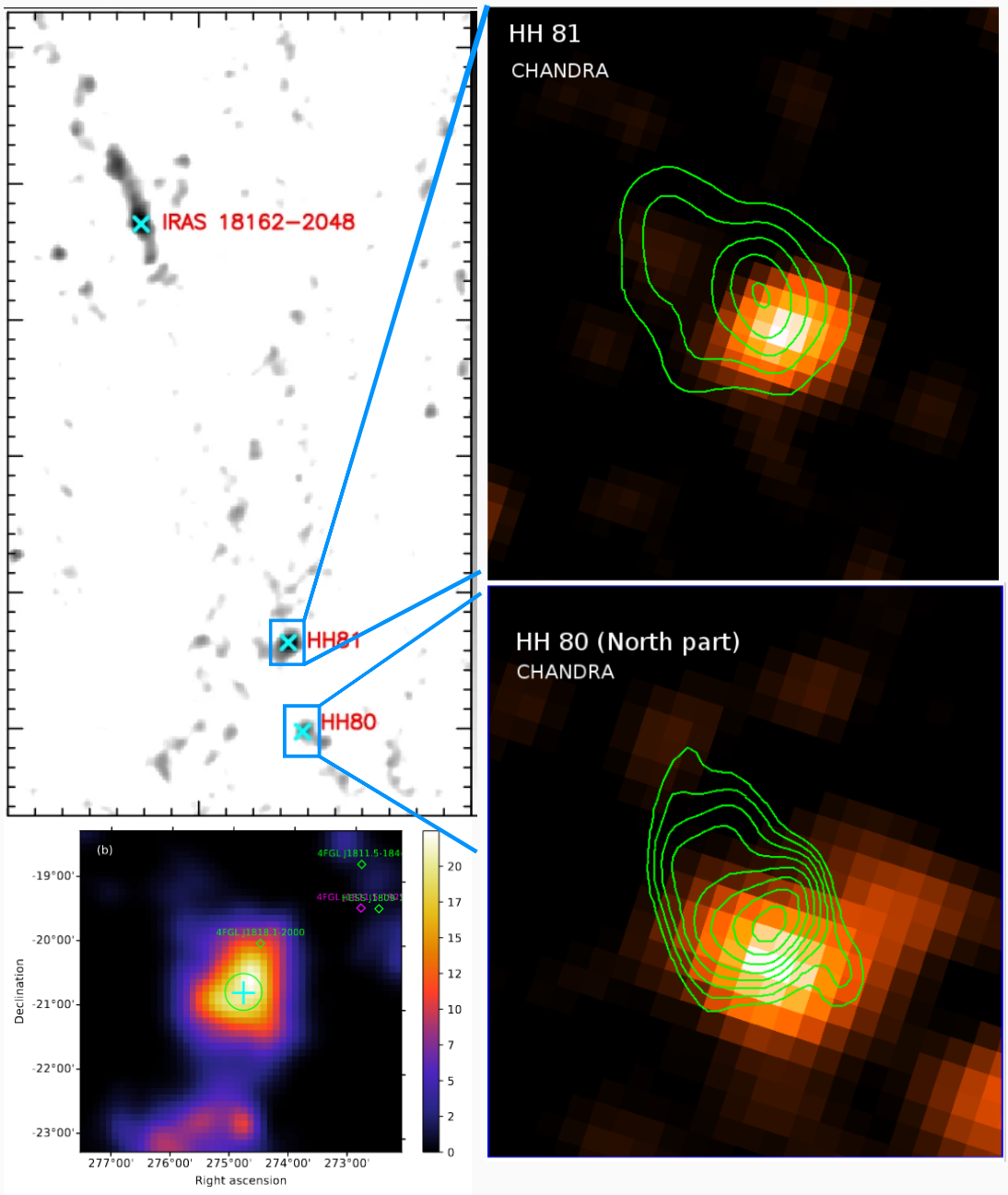

$$\alpha = 0.3$$

$$T \sim 1.3 \times 10^6 \text{ K}$$

$$v_{\rm bs} = 294\sqrt{\frac{T_{\rm ps}}{1.3\times10^6\,{\rm K}}}\ {\rm km\ s^{-1}}$$

$$\frac{d_{\rm th}}{\rm cm} = 3.14\times10^{16}\left(\frac{n_{\rm mc}}{100\,{\rm cm^{-3}}}\right)^{-1}$$

$$R_{\rm HH80} = 5\times10^{16}\ {\rm cm}$$

$$R_{\rm HH81} = 7\times10^{16}\ {\rm cm}$$

Pure synchrotron emission spectral index

$\eta \equiv V_{\rm shell}/V_{\rm X} < 0.03$ for the bow shock to be radiative

$S_{\rm tot} > S_{ff}$ at $\nu = 5.5$ GHz $\Longrightarrow n_{\rm mc} < 10/\sqrt{\eta}$ cm^{-3}

$$\alpha_{\rm nt} = -2.3 \log \left(\frac{0.5 - \eta \left(\frac{n_{\rm shell}}{10^3 {\rm cm}^{-3}} \right)^2}{0.44 - \eta \left(\frac{n_{\rm shell}}{10^3 {\rm cm}^{-3}} \right)^2} \right)$$

$$\boxed{S_{\rm synchr} = S_{\rm tot} - S_{\rm ff}}$$

$$S_{\rm synchr} = A \nu^{\alpha_{\rm nt}}$$

$$\frac{S_{\rm tot}}{\rm mJy} = 0.5 \left(\frac{\nu}{5.5 {\rm GHz}} \right)^{-0.3}$$

$$\frac{S_\nu^{\rm ff}}{\rm mJy} \propto \eta \left(\frac{n_{\rm mc}}{1000 {\rm cm}^{-3}} \right)^2 \left(\frac{\nu}{5.5 {\rm GHz}} \right)^{-0.1}$$

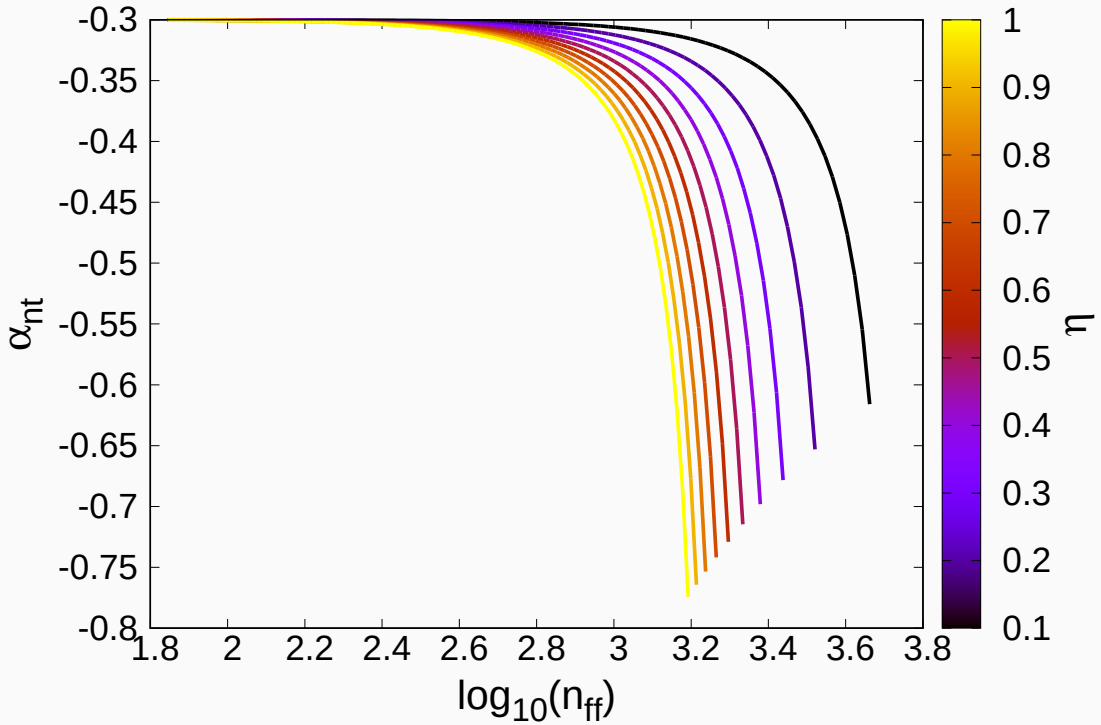

Araudo et al. (in prep.)

Radio to X-rays spectral energy distribution

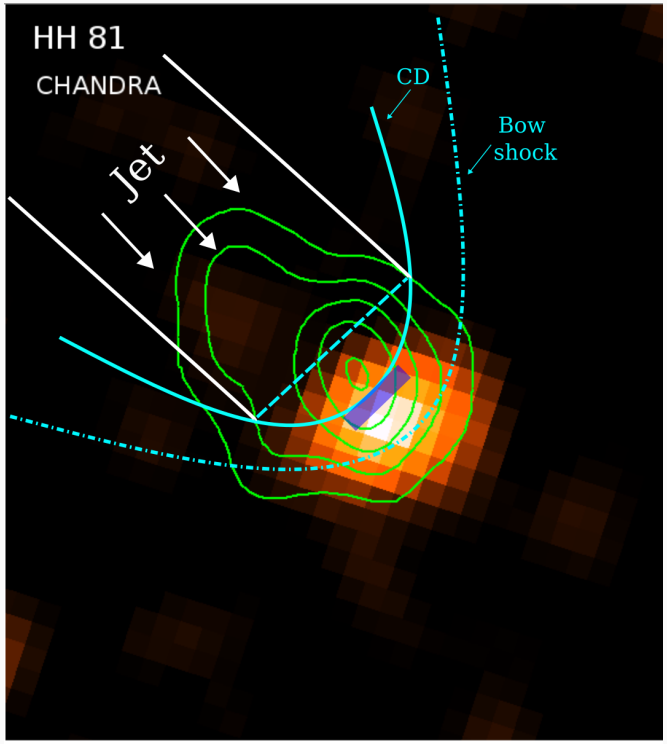

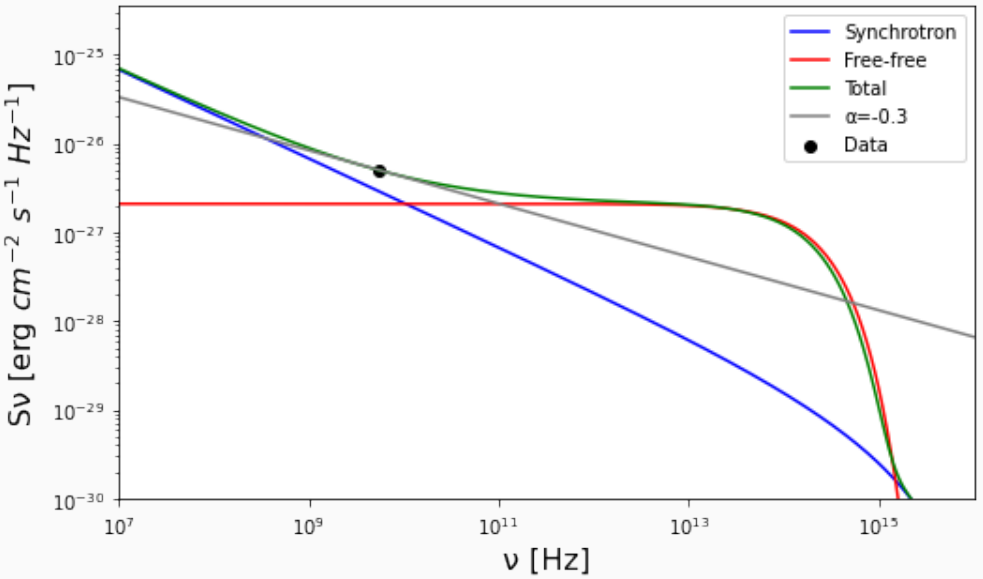

A. Araudo et al. (in prep.)

Gamma-ray emission from S255 NIRS3

S255 NIRS3 ($M_\star \sim 20\ M_\odot$)

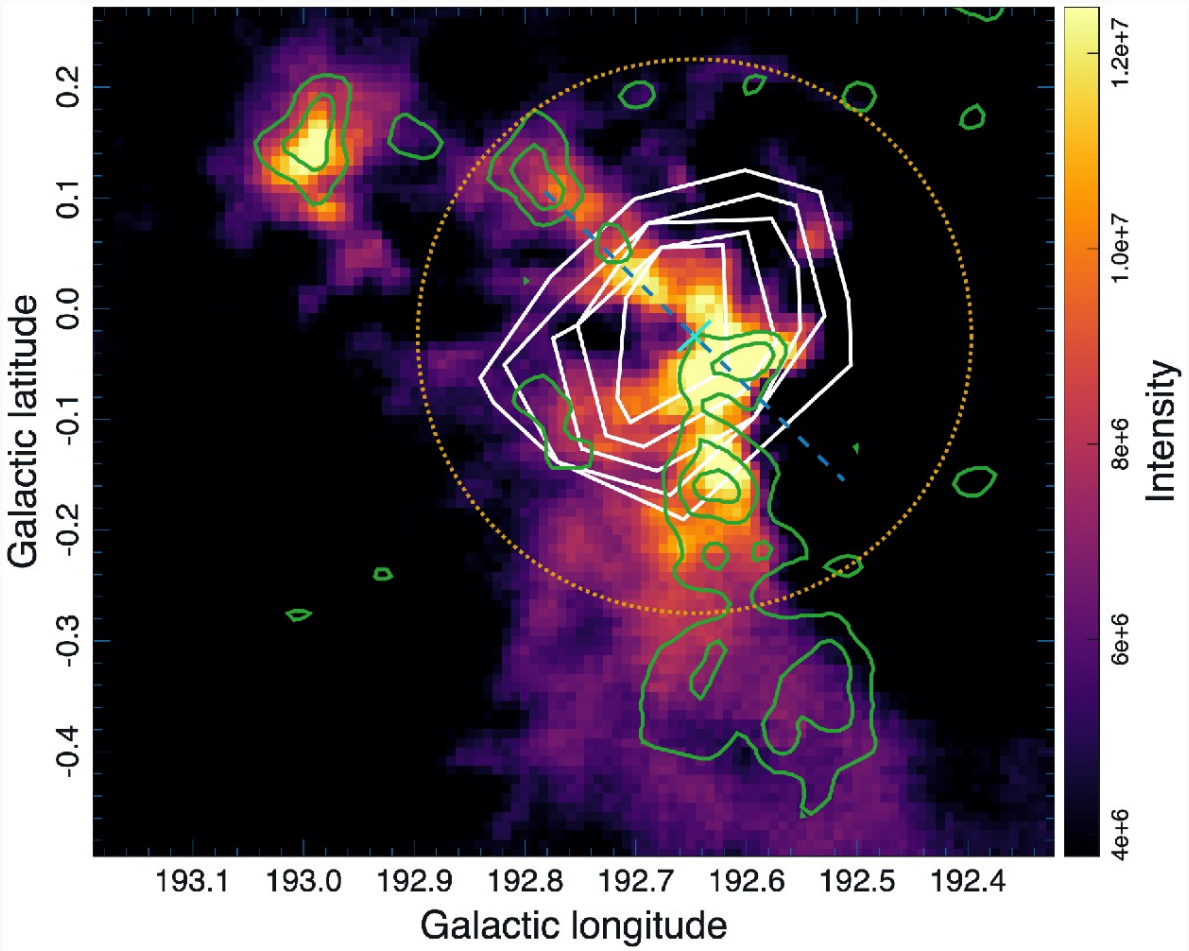

^{13}CO map. Green contours: C^{18}O tracing the two extense filamentary structures. White contours: Fermi above 1 GeV. Blue dashed line: direction of the 1 arcmin molecular bipolar outflow (de Oña Wilhelmi et al. 2023)

Spectral energy distribution

Associated with the Fermi source 4FGL J0613.1+1749c

- $\phi_0 = (6.21 \pm 0.73) \times 10^{13} \mathrm{MeV}^1 \mathrm{cm}^2 \mathrm{s}^1$
- $\alpha = 2.54 \pm 0.07$
- $E_0 = 1.231$ GeV

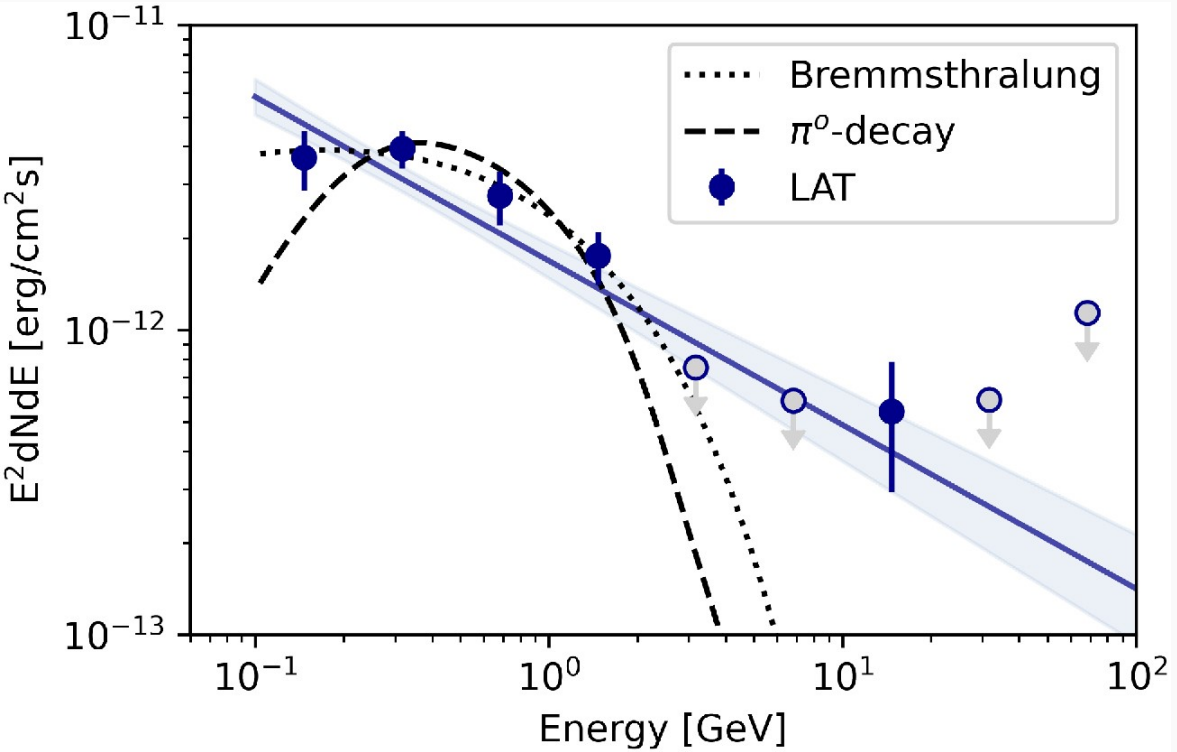

de Oña Wilhelmi et al. (2023)

Currently, only HH80-81 and S255 are GeV emitters

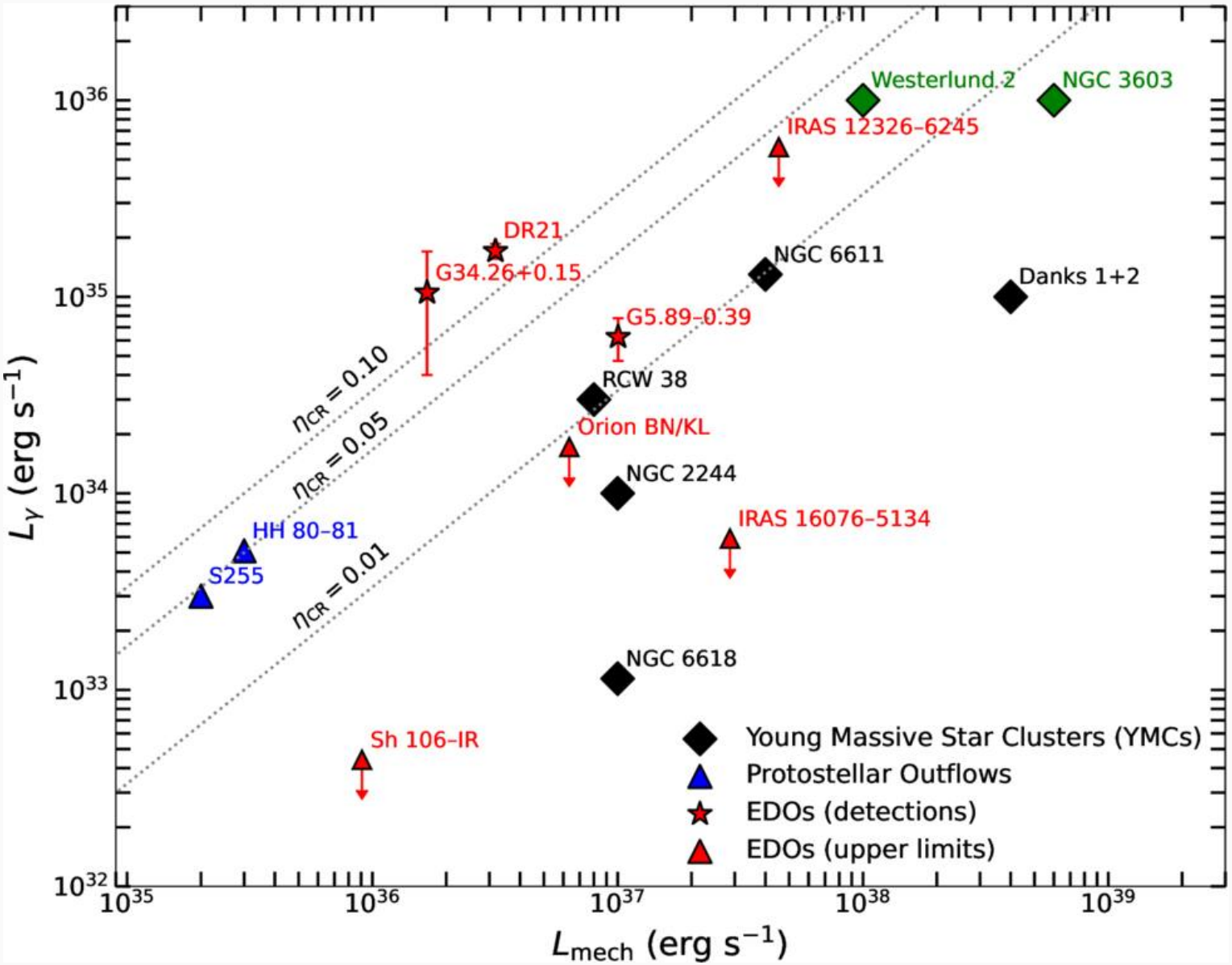

Pandey et al. 2026

Collective and diffuse gamma-ray emission

Massive star formation

Massive stars are formed in groups, in the filaments in molecular clouds (Beuther et al, 2025)

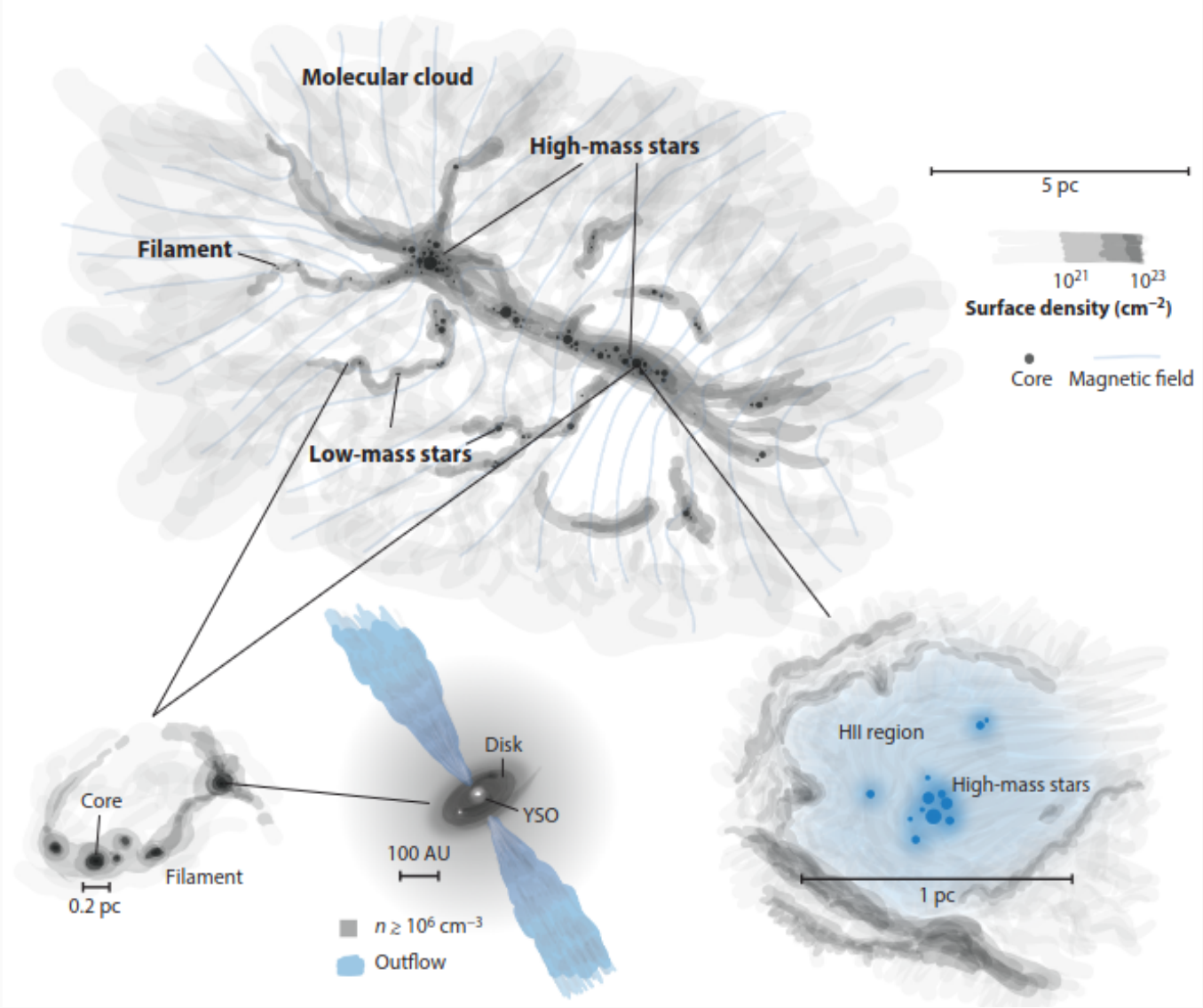

ρ-Ophiuchus star forming region ($d \sim 120$ pc)

Red circles mark four YSOs which drive outflows
Credit: JWST and J. Bally

Collective and diffuse emission

Collective emission

- Jet speed $v_{\rm jet}(m_\star)$
- Jet mass loss rate $\dot{M}_{\rm j}(m_\star) = \eta \dot{M}_{\rm acc}(m_\star)$
- Protostellar mass function $dN/dm_\star$

Diffuse emission Electrons and protons that do not cool down in the jet will escape and radiate in the molecular cloud.

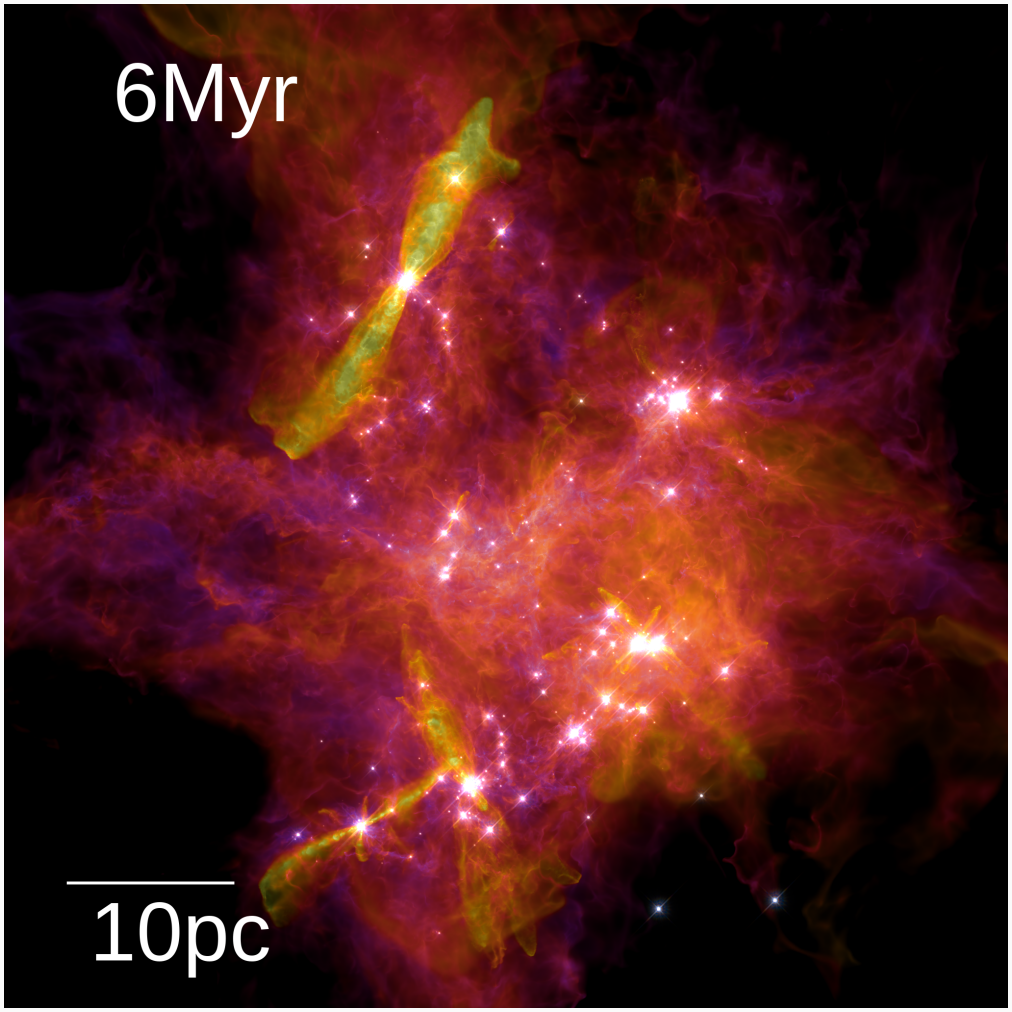

Guszejnov et al. (2020)

These particles can be a source of ionizing cosmic rays

Fermi associations (first catalogue)

Munar-Adrover et al. (2011) found 13 *Fermi* sources being positionally coincident with 24 massive YSOs, and 8 of these *Fermi* sources have not any proposed counterpart (like SNR, PWN, pulsar, etc.)

Fermi Name (1FGL)	RA (°)	Dec (°)	95% Semi major axis (°)	Spectral index Γ ($F \propto E^{-\Gamma}$)	Flux($E > 100$ MeV) $\times 10^{-11}$ erg cm^{-2} s^{-1}	MSX name	RA (°)	Dec (°)	$\Delta\theta$ (°)	Distance* (kpc)	L_{bol}* ($\times 10^3\ L_\odot$)	Mass ($M_\odot$)
J0541.1+3542	85.2805	35.7091	0.1397	2.41 ± 0.13	1.6 ± 0.5	G173.6328+02.8064	85.27929	+35.82633	0.12	1.6[a]	4.8[d]	
						G173.6339+02.8218	85.29592	+35.83380	0.13	1.6[a]	3.2[e]	
						G173.6882+02.7222	85.22758	+35.73558	0.05	1.6[a]	–	
J0647.3+0031	101.8417	0.5289	0.2150	2.41 ± 0.11	1.9 ± 0.5	G212.0641−00.7395	101.80567	+0.43514	0.10	6.4[b]	25[f]	
J1256.9−6337	194.2474	−63.6212	0.1955	2.26 ± 0.12	4.9 ± 1.1	G303.5990−00.6524	194.35546	−63.51650	0.12	11.3[b]	8.3[f]	
J1315.0−6235	198.7635	−62.5971	0.1860	2.31 ± 0.12	6.9 ± 0.0	G305.4840+00.2248	198.40016	−62.53708	0.18	3.6[b]	3.8[f]	
J1651.5−4602	252.8831	−46.0340	0.2258	2.21 ± 0.07	13.9 ± 3.4	G339.8838−01.2588[1]	253.01942	−46.14267	0.14	2.6[b]	21.0[f]	
J1702.4−4147	255.6039	−41.7859	0.0800	2.39 ± 0.07	8.7 ± 2.0	G344.4257+00.0451B	255.53674	−41.78303	0.05	5.0[b]	15.0[f]	
						G344.4257+00.0451C	255.53587	−41.78617	0.05	5.0[b]	15.0[f]	
J1846.8−0233	281.7001	−2.5628	0.1262	2.21 ± 0.06	9.3 ± 2.3	G030.1981−00.1691	281.76274	−2.51003	0.08	7.4[b]	29.0[f]	
J1848.1−0145	282.0470	−1.7605	0.0859	2.23 ± 0.04	9.5 ± 3.2	G030.9726−00.1410	282.09178	−1.80842	0.07	5.7[b]	3.9[f]	1.9×10^3[g]
						G030.9959−00.0771	282.04516	−1,75808	0.0044	5.7[b]	5.1[f]	1.9×10^3[g]
J1853.1+0032	283.2884	0.5366	0.5207	2.18 ± 0.07	5.7 ± 1.7	G032.8205−00.3300	282.04436	−1.75703	0.34	5.1[b]	17.0[f]	
						G033.3891+00.1989	282.89092	+0.49750	0.40	5.1[b]	11.0[f]	
						G033.3933+00.0100	283.06109	+0.41528	0.26	6.8[b]	7.9[e]	
						G033.5237+00.0198	283.11179	+0.53569	0.34	6.8[b]	7.9[e]	
						G034.0126−00.2832	283.60437	+0.83239	0.43	13.3[b]	34.0[f]	
						G034.0500−00.2977	283.63454	+0.85914	0.47	13.3[b]	24.0[f]	
J1925.0+1720	291.2748	17.3485	0.1443	2.28 ± 0.12	2.4 ± 1.0	G052.2025+00.7217A	291.24933	+17.42169	0.08	10.2[b]	15.0[f]	
						G052.2078+00.6890	291.28553	+17.41317	0.07	10.2[b]	20.0[f]	
J1943.4+2340	295.8667	23.6815	0.1118	2.23 ± 0.11	2.6 ± 0.7	G059.7831+00.0648[2,3]	295.79680	+23.73433	0.08	2.2[a]	6.8[f]	840 and 190 [h]
J2040.0+4157	310.0154	41.9533	0.1970	2.66 ± 0.06	7.9 ± 1.2	G081.5168+00.1926	309.99066	+41.98739	0.04	1.7[c]	0.704[f]	

Conclusions

- Synchrotron emission evidence the presence of relativistic electrons MYSO jets.
- Jets from high mass protostars (velocities ~ 500 km s^{-1} and densities $\sim 100 - 10^4$ cm^{-3}) have enough kinetic power to accelerate particles and destabilise non-resonant (Bell) modes
- Rayleigh-Taylor mixing can make protostellar jets detectable in the gamma-ray domain
- HH80/81 and S255 NIRS3 are currently the only two protostellar jets associated with *Fermi* sources.

The detection of gamma rays from protostellar jets is very important to study DSA and magnetic field amplification in the high-density and low-velocity regime

Questions?

Polarization measurements

Polarization measurement in IRAS 18162 (Herbig-Haro objects HH80 and HH81)

- Low spatial resolution VLA data (C-configuration)
- Magnetic field parallel to the jet axis
- Equipartition magnetic field $\sim$ 0.2 mG

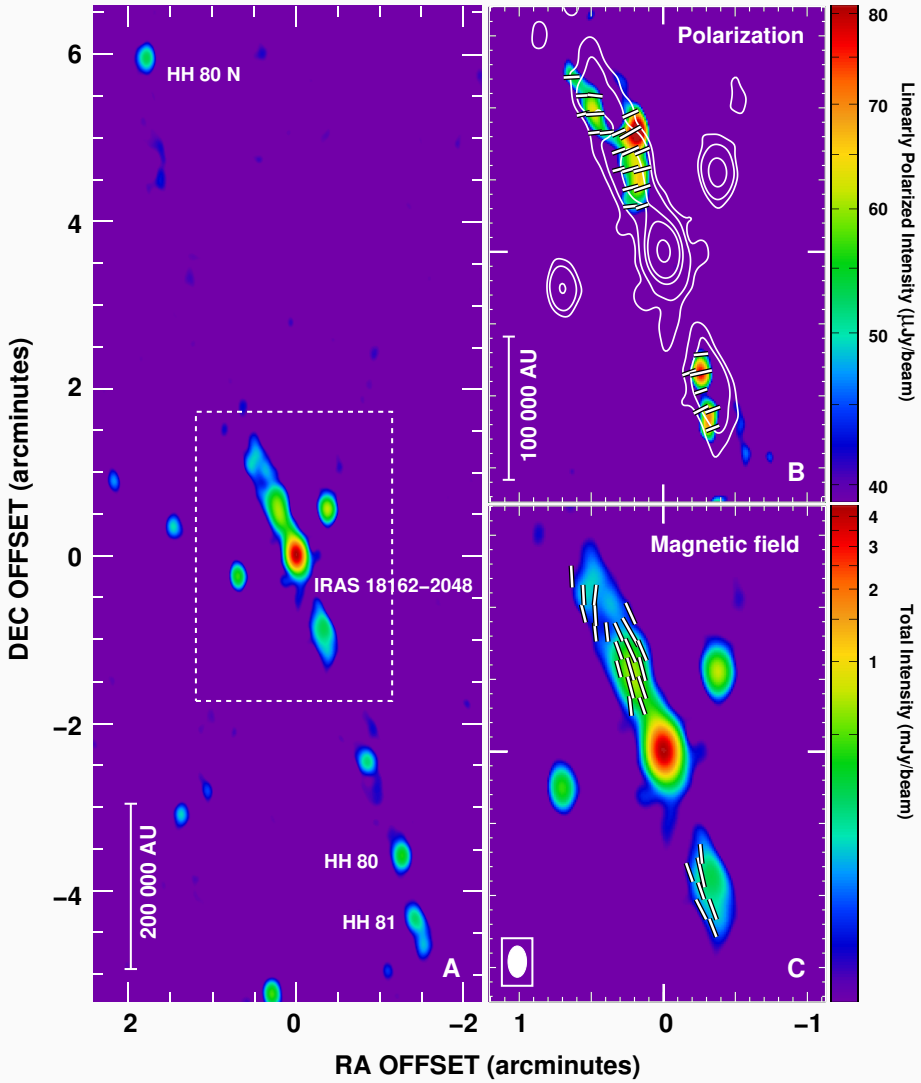

Carrasco-Gonzalez et al. (2010)

Magnetic fields

Scalling law $B_j \propto n_j^{\beta}$
$0.5 < \beta < 1$

AVERAGE JET PARAMETERS

Distance from Star (AU)	Arcseconds[a]	n[b] (cm^{-3})	$B_\perp$	V_A[c] (km s^{-1})
10	0.02	2.5×10^6	82 mG	113
30	0.06	1.5×10^6	53 mG	94
100	0.2	4.5×10^5	19 mG	62
300	0.6	8.8×10^4	4.8 mG	35
10^3	2.2	10^4	0.75 mG	16
3×10^3	6.5	1.2×10^3[d]	124 μG[d]	7.8
10^4	22	110[d]	16 μG[d]	3.3
3×10^4	65	12[d]	2.4 μG[d]	1.5

Hartigan et al. (2007)

Equipartition magnetic fields in synchrotron jets: $B_{eq} \sim 100 - 500\,\mu$G $\Rightarrow B_{eq} \sim 100 B_j \Rightarrow$ Magnetic field amplification?

$B_{eq} \sim 100\,\mu\text{G} \Rightarrow U_p > U_e \sim 10^{-8}(B_{eq}/500\,\mu\text{G})$ erg cm$^{-3} \Rightarrow$ Local particle acceleration! (Padovani et al. 2016, Fontani et al. 2017)

HH 81 (Radio + X-rays)

Shift between radio and X-ray emission (peak possition)

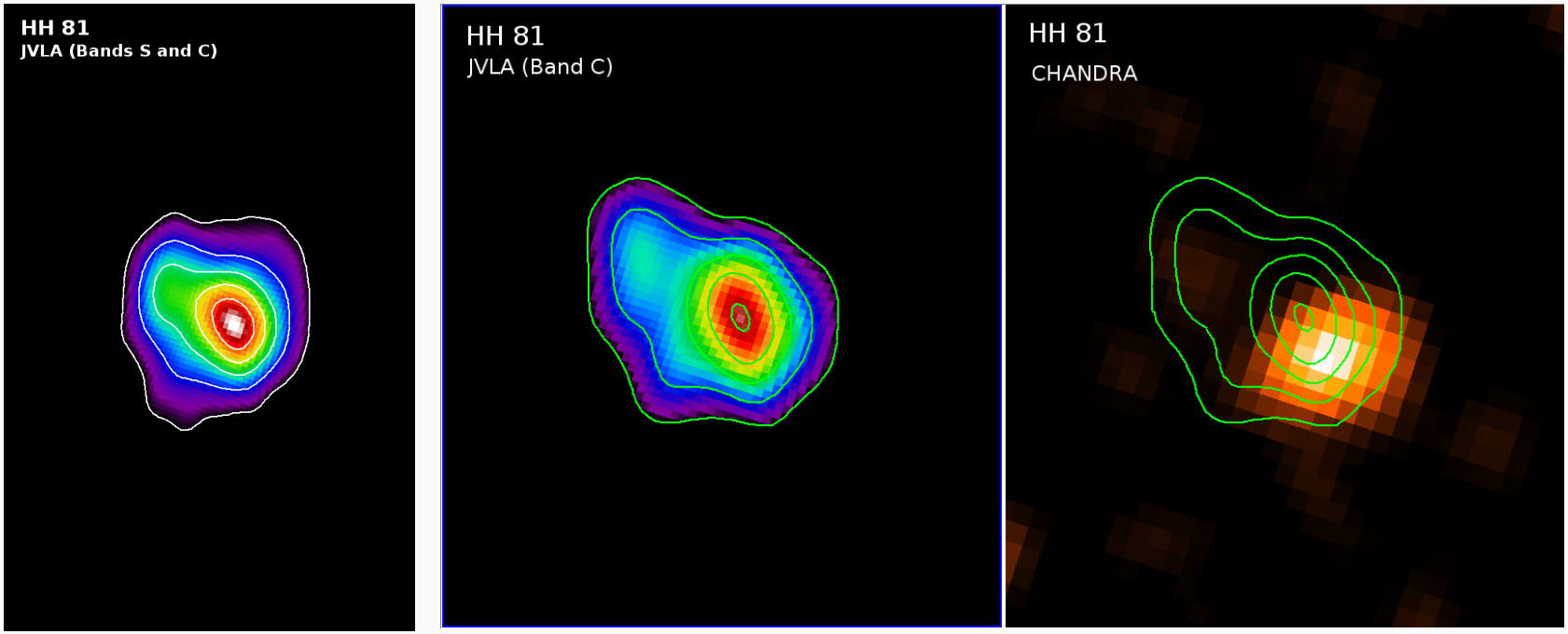

Rodríguez-Kamenetzky et al. (2019)

HH 80 (Radio + X-rays)

Shift between radio and X-ray emission (peak possition)

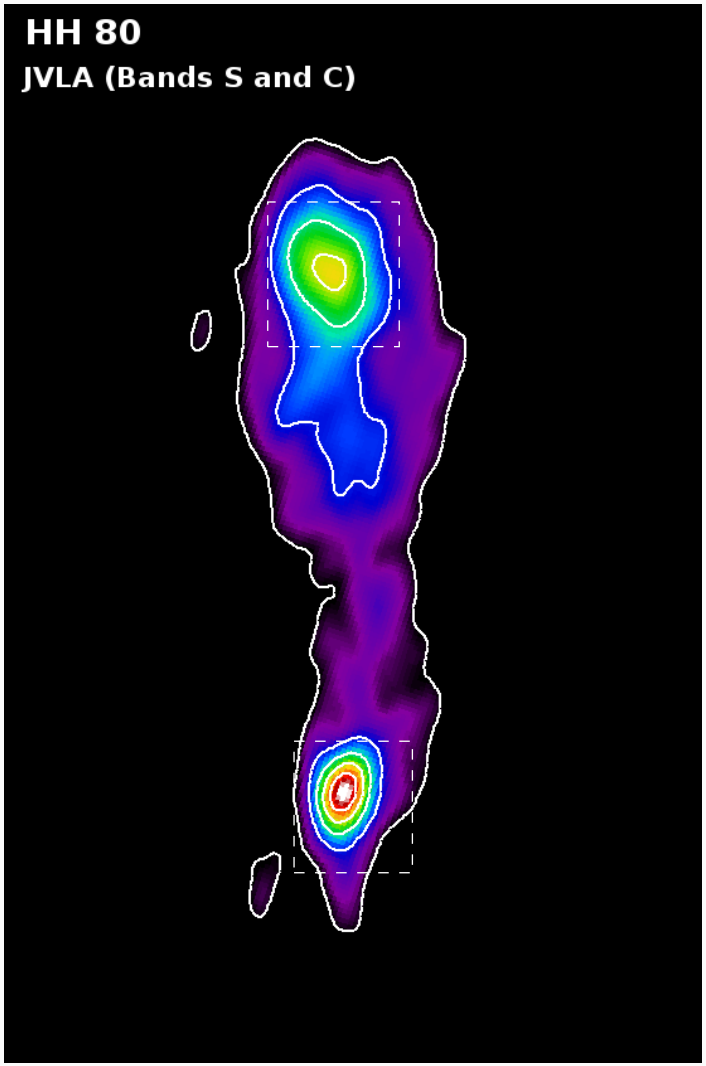

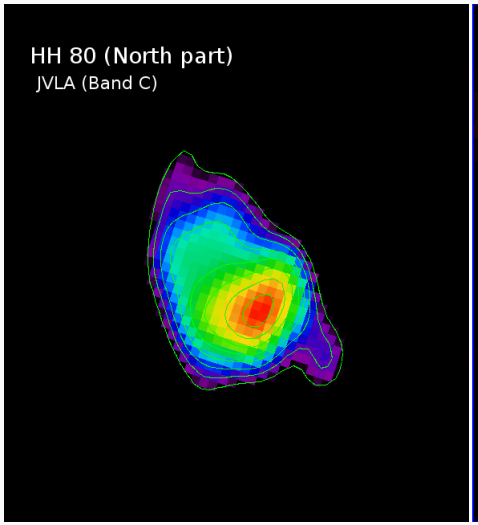

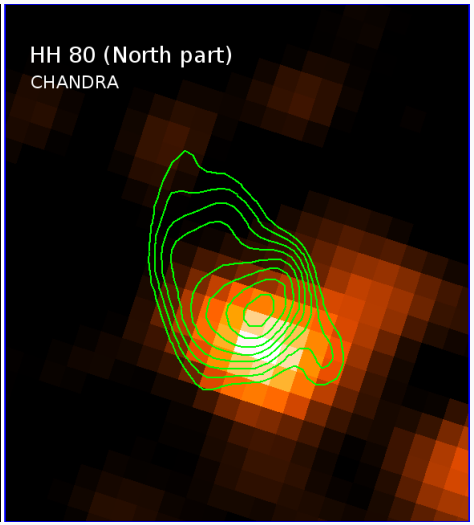

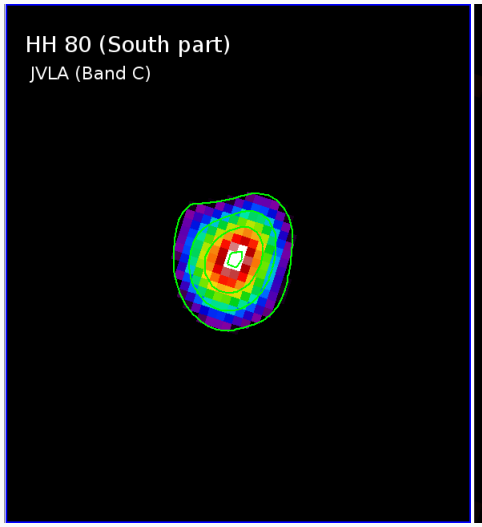

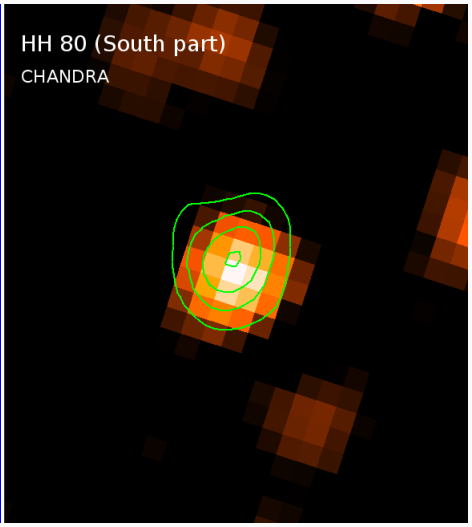

Rodríguez-Kamenetzky et al. (2019)

HH 80: Non-thermal X-ray emitter?

Synchrotron origin of the X-rays (light-blue in the figure) was claimed by López Santiago et al. (2013)

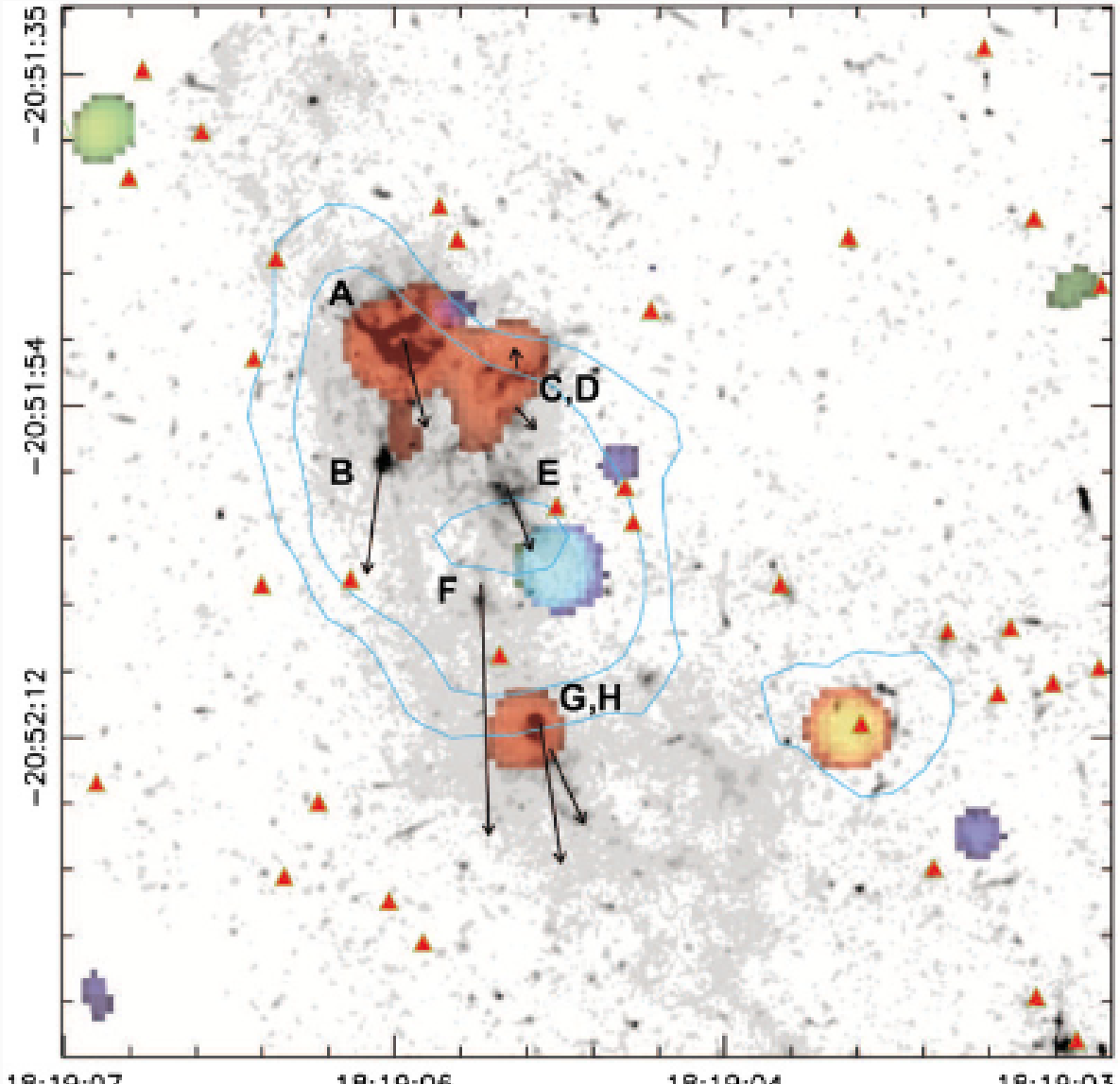

Maximum energy of non-thermal particles

- Bell (non-resonant)

$$\Gamma_{\rm max-NR} \sim \eta_{\rm cr} M_{\rm A}$$

- Alfvén (resonant)

$$\Gamma_{\rm max-RES} \sim r_{\rm g}^{-1} \sqrt{\frac{\eta_{\rm cr} V_{\rm sh}^3}{c}}$$

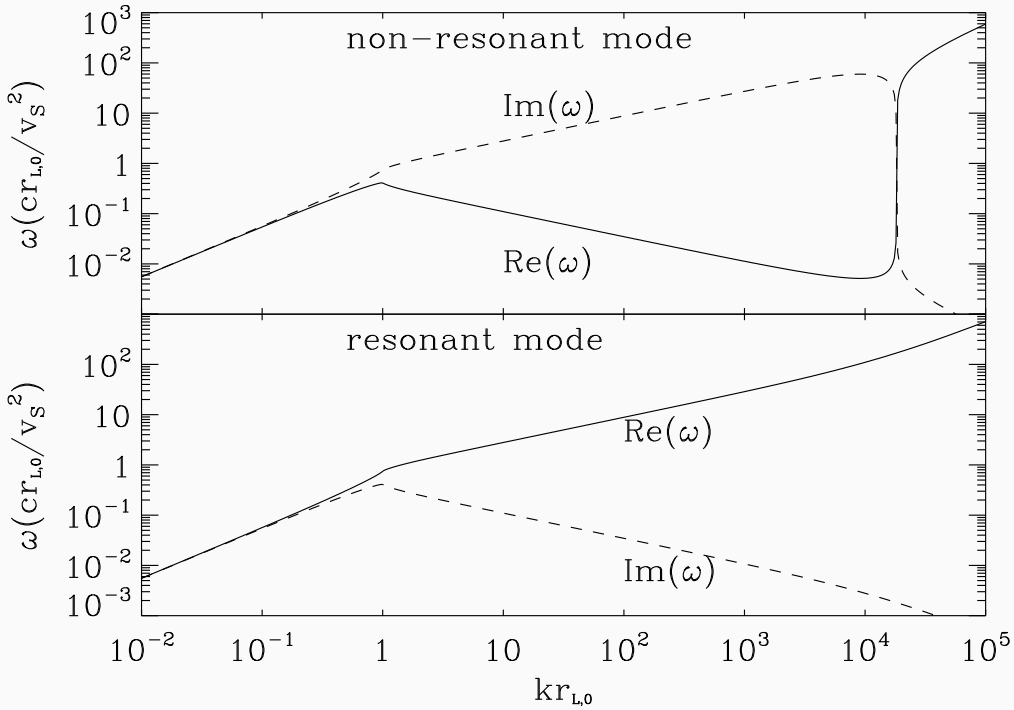

Amato & Blasi (2009)

$$\boxed{\Gamma_{\rm max-NR} > \Gamma_{\rm max-RES}}$$

$t_{\rm acc} \sim \frac{1}{\Gamma_{\rm max}} \Rightarrow$ in the Bell regime particles achieve higher energies in the available time

Cosmic-ray streaming instabilities

Dispersion relation

$$\omega^2 - k^2 v_{\rm A}^2 - k\zeta \frac{v_{\rm sh}^2}{r_{\rm gm}} = 0$$

- Alfvén (resonant): $k^2 v_{\rm A}^2 > k\zeta \frac{v_{\rm sh}^2}{r_{\rm gm}}$
- Bell (non resonant): $k^2 v_{\rm A}^2 < k\zeta \frac{v_{\rm sh}^2}{r_{\rm gm}}$

  Magnetic field amplification!

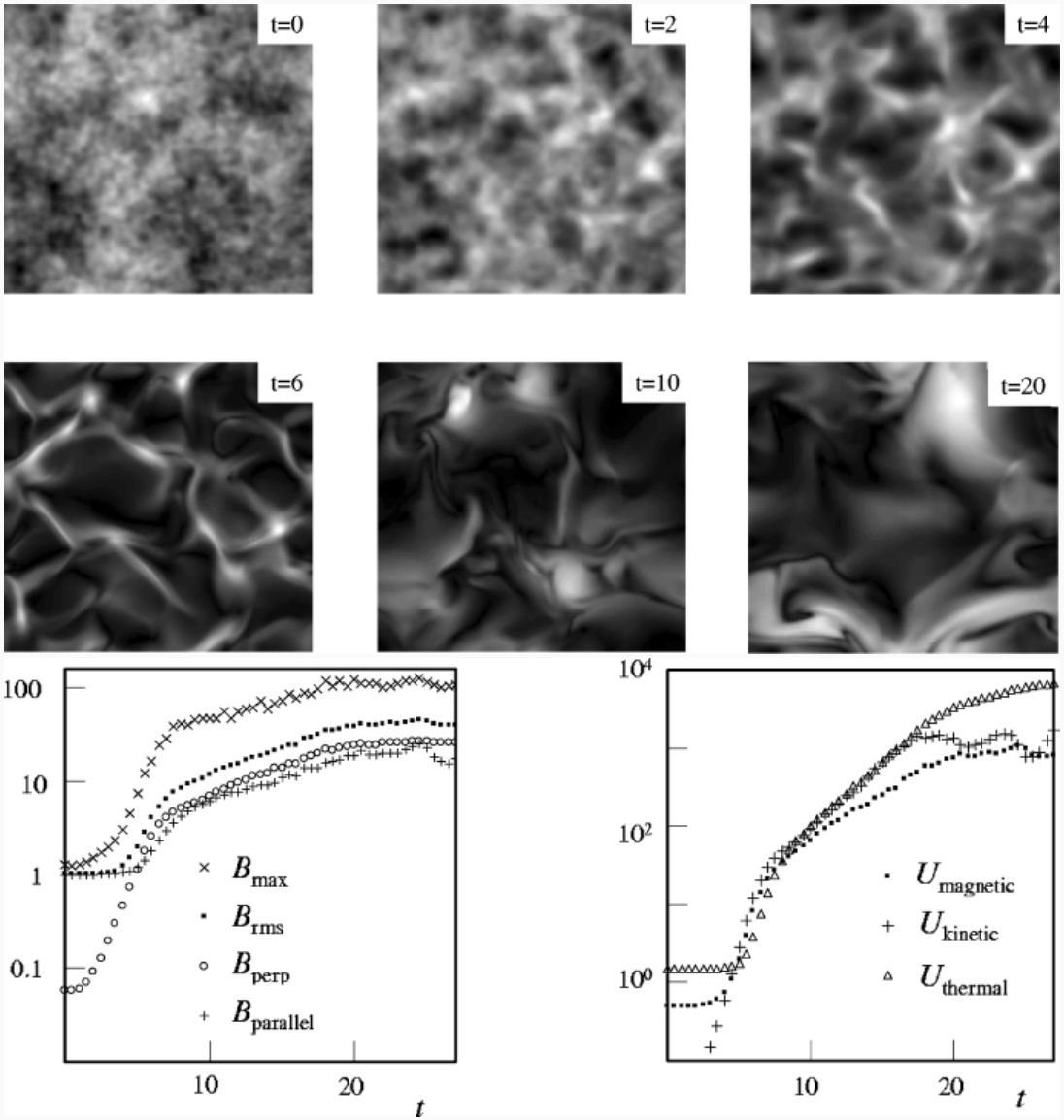

Bell (2004, 2005)